HHS Public Access

Author manuscript

Dev Cell. Author manuscript; available in PMC 2021 October 26.

Published in final edited form as:

Dev Cell. 2020 October 26; 55(2): 133–149.e6. doi:10.1016/j.devcel.2020.07.015.

Metabolic regulation of inflammasome activity controls embryonic hematopoietic stem and progenitor cell production

Jenna M. Frame[1], **Caroline Kubaczka**[1], **Timothy L. Long**[1], **Virginie Esain**[1], **Rebecca A. Soto**[1,2], **Mariam Hachimi**[1], **Ran Jing**[1], **Arkadi Shwartz**[3], **Wolfram Goessling**[2,3,4,5], **George Q. Daley**[1,2,5,6], **Trista E. North**[1,2,5,*]

[1]Stem Cell Program, Department of Hematology/Oncology, Boston Children's Hospital, Boston, MA, 02115, USA

[2]Developmental and Regenerative Biology Program, Harvard Medical School, Boston, MA, 02115, USA

[3]Genetics Division, Brigham & Women's Hospital, Boston, MA, 02115, USA

[4]Gastroenterology Division, Massachusetts General Hospital, Boston, MA, 02114, USA

[5]Harvard Stem Cell Institute, Harvard University, Cambridge, MA, 02138, USA

[6]Department of Biological Chemistry and Molecular Pharmacology, Harvard Medical School, Boston, MA, 02115, USA

Summary

Embryonic hematopoietic stem and progenitor cells (HSPCs) robustly proliferate while maintaining multilineage potential *in vivo*; however, an incomplete understanding of spatiotemporal cues governing their generation has impeded robust production from human induced pluripotent stem cells (iPSCs) *in vitro*. Using the zebrafish model, we demonstrate that NLRP3 inflammasome-mediated interleukin-1-beta (IL1β) signaling drives HSPC production in response to metabolic activity. Genetic induction of active IL1β or pharmacologic inflammasome stimulation increased HSPC number as assessed by *in situ* hybridization for *runx1/cmyb* and flow cytometry. Loss of inflammasome components, including *il1b*, reduced $CD41^{+}$ HSPCs, and prevented their expansion in response to metabolic cues. Cell ablation studies indicated that macrophages were essential for initial inflammasome stimulation of $Il1rl1^{+}$ HSPCs. Significantly, in human iPSC-derived hemogenic precursors, transient inflammasome stimulation increased multilineage hematopoietic colony-forming units and T-cell progenitors. This work establishes the

[*]**Corresponding Author/Lead Contact:** Trista.North@childrens.harvard.edu.

Author Contributions

JMF and VE conceived the study and generated the *Tg(hsp70l:il1b)* line. MH performed EdU studies, imaging analyses, and assisted with cloning. AS performed time-lapse imaging. JMF, TLL, VE, and RAS performed all other zebrafish experiments. RJ performed human iPSC T cell differentiation; CK performed all other iPSC experiments. WG, GQD and TEN analyzed data and provided guidance. JMF wrote and TEN edited the manuscript.

inflammasome as a conserved metabolic sensor that expands HSPC production *in vivo* and *in vitro*.

eTOC:

Frame et al. identify an integral role for the inflammasome in stimulating *de novo* production of zebrafish and human hematopoietic stem and progenitor cells (HSPCs). Inflammasome-associated IL1β signaling is induced *in vivo* by developmental metabolic cues and relayed from primitive macrophages to hemogenic endothelium to promote embryonic HSPC formation.

Graphical Abstract

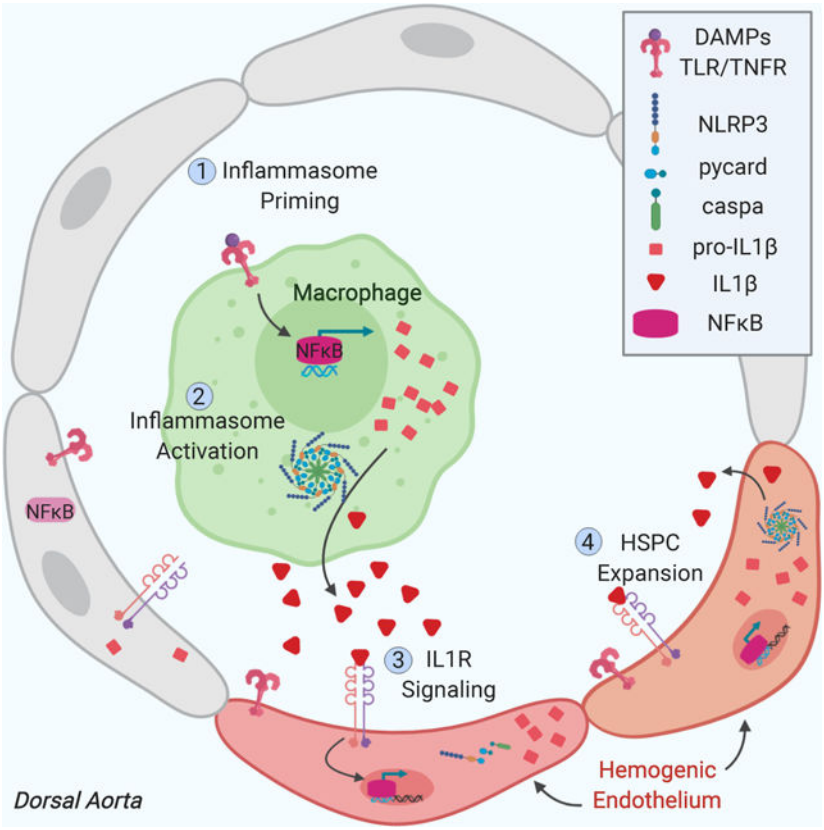

Keywords

Inflammasome; Hematopoietic Stem Cell (HSC); IL1β; endothelial-to-hematopoietic transition (EHT); zebrafish; inflammation; iPSC; Nlrp3

Introduction

Hematopoietic stem and progenitor cell (HSPC) transplantation can be used as a curative treatment in individuals with hematologic disorders or malignancies. However, these therapies depend on donor HSPC abundance and histocompatibility, thereby restricting their application. Improving HSPC generation from autologous pluripotent cell sources could

overcome this limitation. Currently, attempts to derive *bona fide* human HSPCs from induced pluripotent stem cells (iPSCs) require genetic manipulation to induce robust expansion and achieve long-term multilineage engraftment in murine models (Daniel et al., 2016; Sugimura et al., 2017). Further elucidation of conserved spatiotemporal regulators of HSPC specification and expansion acting *in vivo* in model systems are necessary for the optimization of *in vitro* cultures for therapeutic use. Here, we describe a connection between metabolic state and sterile inflammatory signaling that regulates HSPC production through inflammasome activity in the zebrafish embryo. Furthermore, we demonstrate conservation of inflammasome activation in modulating expansion and multipotency of human iPSC-derived HSPCs.

The ontogeny of the vertebrate hematopoietic system is a complex yet tightly orchestrated process. Several highly conserved “waves” of hematopoietic cells emerge over developmental time, with each becoming increasingly diverse in terms of lineage potential and expansion capabilities (Dzierzak and Speck, 2008; Medvinsky et al., 2011; Clements and Traver, 2013). Initial waves of primitive erythroid and myeloid-restricted progenitors are closely followed by bipotent erythro-myeloid progenitors and lymphoid-restricted progenitors formed in the posterior blood island and caudal aortic endothelium of the zebrafish (Bertrand et al., 2007; Tian et al., 2017), and the yolk sac of murine and human embryos (McGrath et al., 2015; Böiers et al., 2013; Ivanovs et al., 2017). Finally, hematopoietic stem cells with extensive self-renewal and multilineage differentiation capacity arise from a subset of “hemogenic” endothelium lining the embryonic dorsal aorta in all vertebrates. In the zebrafish aorta, commitment of phenotypic endothelium to hemogenic fate is signified by the step-wise acquisition of *gata2b* expression, which in turn upregulates *runx1* expression around 24 hours post fertilization (hpf) (Butko et al., 2015). Subsequently, individual Runx1^{+} cells acquire rounded, hematopoietic morphology, and egress from the ventral wall through a process termed “endothelial-to-hematopoietic transition” (EHT) (Bertrand et al., 2010; Kissa and Herbomel, 2010; Lam et al., 2010). The majority of Runx1-dependent HSPC “budding” initiates from 30–36hpf, followed by egress from the endothelium from 40–52hpf (Kissa and Herbomel, 2010). HSPCs subsequently migrate to the caudal hematopoietic tissue (CHT), and eventually, the thymus and kidney marrow to expand and differentiate. There is increasing evidence that the initial populations of embryonic hematopoietic cells provide instructive cues to trigger HSPC production. For example, sterile inflammatory cytokine signaling promotes formation of zebrafish and murine HSPCs during embryonic development, independently of infection or injury (Orelio et al., 2008, 2009; Li et al., 2014; Sawamiphak et al., 2014; Espín-Palazón et al., 2014; He et al., 2015). Both macrophages (Li et al., 2014; Mariani et al., 2019) and neutrophils (Espín-Palazón et al., 2014) have been identified as sources of inflammatory cues. However, it remains unclear how these accessory cell types initiate inflammatory cascades to specify and/or amplify embryonic HSPC production.

One of the master regulators of inflammation, IL1β, directs adult HSPCs to divide, and promotes emergency granulopoiesis and T cell activation through signaling of downstream cytokines (Dinarello, 2009, 2011; Pietras et al., 2016). Although the acute effects of IL1β in infection and immunity are typically beneficial, chronic inflammation can be detrimental to adult HSC maintenance, thus, inflammatory signals must be tightly modulated to maintain

optimal physiologic responses (Essers et al., 2009; Baldridge et al., 2010; King and Goodell, 2011; Takizawa et al., 2011; Esplin et al., 2011). Typically sourced in large quantities by myeloid cells, especially macrophages, IL1β activity is controlled at the protein level by inflammasomes (Dinarello, 2009). These multimeric complexes are generally comprised of one member of a family of Nod-like pattern recognition receptors (NLR), the adapter protein Pycard, and Caspase1, which autoactivates and cleaves IL1β and a related cytokine IL18, in response to a variety of microbial and host-derived stimuli (He et al., 2016; Jo et al., 2016). Inflammasome-forming proteins are present in zebrafish (Masumoto et al., 2003; Kuri et al., 2017; Li et al., 2018), and zebrafish Caspase a (Caspa) has the ability to cleave IL1β (Vojtech et al., 2012). Inflammasome activation *in vitro* involves two sequential steps: a "priming" signal, usually mediated by Toll-like Receptor (TLR) activation, resulting in transcriptional activation of NFκB and synthesis of IL1β and NLR proteins, followed by a second "activation" signal, which is responsible for assembly and activation of caspase-1 to cleave IL1β into its active form (He et al., 2016; Jo et al., 2016). *In vivo*, exogenous induction of inflammasome priming is not usually required for pharmacologic activators to generate a response (Rock et al., 2010). Intriguingly, both TLR signaling and NFκB were previously shown to be active in developing HSPCs (Espín-Palazón et al., 2014; He et al., 2015), suggesting that sterile inflammasome "priming" occurs normally during embryogenesis.

The most well-studied inflammasome, NLRP3, is often associated with metabolic alterations in adult pathologies, such as type 2 diabetes and atherosclerosis (Lee et al., 2013; Patel et al., 2017; Hughes and O'Neill, 2018). In this context, inflammasome activation and subsequent IL1β production can be induced by heightened sterile "danger" signals, including elevations in the glycolytic enzyme hexokinase, reactive oxygen species (ROS), and cholesterol deposits (Moon et al., 2015; Duewell et al., 2010; Camell et al., 2015; Abderrazak et al., 2015). Priming of the NLRP3 inflammasome is reliant on glycolysis and HIF1α stabilization in adult macrophages (Masters et al., 2010; Tannahill et al., 2013), and is enhanced in response to high glucose concentrations or hypoxia in mesangial cells (Tseng et al., 2016). In mice, macrophages increase IL1β secretion after normal feeding (Dror et al., 2017). Adult HSPCs are also capable of inflammasome activation, as murine HSPCs with hyperactive Nlrp1a have compromised function (Masters et al., 2012). However, whether the inflammasome responds to metabolic cues to regulate embryonic HSPC production is undetermined.

We previously established that glucose metabolism expands HSPC formation in zebrafish embryos through elevated ROS generation and HIF1α-mediated induction of key hematovascular genes and signals (Harris et al., 2013; Lim et al., 2017). While HIF1α activation can induce *il1b* transcription in developing zebrafish macrophages (Ogryzko et al., 2019), a connection between energy metabolism and sterile inflammasome activity in the context of HSPC formation has not been explored. Here, we provide evidence that metabolic alterations promote inflammasome-induced IL1β signaling to enhance HSPC production, which has implications for future efforts to derive functional human HSPCs *de novo* for therapeutic application.

Results

Metabolic stimulation induces inflammasome priming in the embryo

We previously demonstrated that metabolic stimulation promotes HSPC formation in zebrafish embryos via ROS-mediated HIF1α stabilization. In addition to a HIF1α signature, prior transcriptional analyses indicated that a strong inflammatory response was induced by glucose metabolism (Harris et al., 2013). Quantitative PCR (qPCR) analyses confirmed that exogenous glucose (12hpf) globally induced *il1b* at 24hpf and 36hpf, during the time of HSPC production (Fig. 1A, Fig. S1A). This induction was more pronounced after prolonged glucose exposure, and also resulted in substantial increases in expression of *tnfa* (Sieger et al., 2009) and *il6,* cytokines previously found to promote embryonic HSPC specification (Espín-Palazón et al., 2014; Lim et al., 2017)(Fig. 1B). Increased *il1b* expression was similarly observed following exposure to ROS during HSPC specification (12–36hpf) (Fig. 1C), or stabilization of HIF1α with $CoCl_2$ treatment (24–120hpf) (Fig. S1B) (Harris et al., 2013). These data indicate that *il1b* transcripts are induced by activation of the glucose-ROS-HIF axis, and suggest that metabolic cues may prime embryos for HSPC formation and/or expansion through production of inflammatory cytokines.

To determine if IL1β function is required to mediate the effects of glucose metabolism on HSPC formation, morpholino-mediated knockdown of *il1b* was performed in the context of glucose exposure. Consistent with our prior observations (Li et al., 2014), *il1b* morphants (López-Muñoz et al., 2011) exhibited a reduction in expression of HSPC markers *runx1/cmyb* by whole-mount *in situ* hybridization (WISH), and generated fewer $CD41^+$ HSPCs in *Tg(−6.0itga2b:egfp)* embryos (Harris et al., 2013; Li et al., 2015; Ma et al., 2011) when compared with controls at 48hpf (Fig. 1D–E, Fig. S1C–E). Furthermore, this deficit partially prevented glucose from inducing *runx1/cmyb* expression and HSPC number, suggesting that IL1β is required to promote HSPC expansion in the setting of increased glucose bioavailability.

To examine whether endogenous glucose fluctuations in the zebrafish embryo may promote sterile inflammatory signaling in the absence of exogenous metabolic stimulation, glucose levels were measured at frequent intervals throughout HSPC specification. Intriguingly, embryonic glucose levels tripled between 18 and 30hpf (Fig. 1F), consistent with prior observations, and coincident with the developmental onset of gluconeogenesis in zebrafish embryos (Dhillon et al., 2019; Jurczyk et al., 2011). To determine whether endogenous glucose production was temporally correlated with inflammasome priming, expression of inflammasome components in the embryo were assayed. Expression of *nlrp3l, caspa,* and *pycard* increased over the same developmental time (Fig. 1G), suggesting that inflammasome complexes become functional during the window of HSPC specification. Analysis of *Tg(il1b:EGFP)* embryos (Hasegawa et al., 2017) demonstrated EGFP co-expression with primitive macrophages in *Tg(mfap4:tdtomato)* embryos (Walton et al., 2015), both in circulation and closely associated with the aortic endothelium (Fig. S1F), as well as the endothelium itself in *Tg(flk1:mCherry)* embryos at 36hpf (Hogan et al., 2009) (Fig. 1H). Furthermore, FACS-isolated Il1β:$EGFP^+$ cells expressed markers indicative of macrophage (*mpeg1*), neutrophil (*mpx*) and HSPC and/or thrombocyte (*CD41*) identity by

PCR (Fig. S1G). Together, these data imply that inflammasome-derived IL1β signaling (Fig. 1I) is primed by metabolic cues, and is active in cell populations that are temporally and spatially associated with HSPC formation.

Inflammasome complexes are necessary for normal HSPC generation

After transcriptional priming of *il1b* and inflammasome components, pro-IL1β protein is cleaved and activated by multimeric inflammasome complexes in response to sterile or microbial stimuli (Fig. 1I). To determine if inflammasome components are functionally required during HSPC formation, targeted knockdown studies were performed. Disruption of the effector *caspa* (Masumoto et al., 2003) substantially reduced *runx1/cmyb* expression by WISH (Fig. 2A–B; Fig. S2A–B), and glucose exposure failed to increase HSPC gene expression in morphant embryos. This decrease was not associated with alterations in arterial specification, as *efnb2* expression was unchanged in morphants, but notably, expression of the hemogenic marker *gata2b* was reduced (Fig. S2C–D). A significant reduction of $CD41^+$ HSPCs in *caspa* morphants was quantified by flow cytometry (Fig. 2C). While transient caspase inhibition with non-toxic doses of Ac-YVAD-CMK only caused a trend toward diminished *runx1/cmyb* expression (Fig. S2E), consistent with prior reports (Tyrkalska et al., 2019), analysis of $caspa^{-/-}$ embryos (Kuri et al., 2017) demonstrated a reduction of *runx1/cmyb* in the aorta (Fig. 2D–E), with mutants exhibiting a blunted response to glucose exposure (Fig. S2F). Fewer $CD41^+$ HSPCs were also enumerated in the CHT of $caspa^{-/-}$ embryos compared with wild-type clutchmates (Fig. 2F–G).

To confirm that these effects on HSPC development were due to loss of sterile inflammasome function, additional components of the complex were targeted. Knockdown of the adapter *pycard* (Progatzky et al., 2014) (Fig. S2G) significantly decreased *runx1/cmyb* expression by WISH and numbers of $Flk1^+cMyb^+$ HSPCs in *Tg(flk1:dsRed;cmyb:EGFP)* embryos (Bertrand et al., 2010; Kikuchi et al., 2011; North et al., 2007) assessed by flow cytometry (Fig. 2H–I). A reduction in *runx1/cmyb,* as well as numbers of $CD41^+$ HSPCs, was also observed in *pycard* mutants (Matty et al., 2019) compared to $pycard^{+/+}$ embryos (Fig. 2J–K). A large family of putative NLR sensor genes have been identified in zebrafish (Laing et al., 2008); knockdown of a predicted sensor gene *nlrp3l* phenocopied *caspa* and *pycard* morphants with reduced *runx1/cmyb* in the aorta at 36hpf (Fig. 2L–M, Fig. S2H–J). *Rag1* expression, indicative of reduced or delayed HSPC colonization in the thymus, was also decreased in *nlrp3l* morphants (Fig. S2K–L). Fewer $CD41^+$ HSPCs were detected in *nlrp3l* morphants, as well as in embryos in which a newly annotated and characterized *nlrp3* gene was targeted (Li et al., 2020)(Fig. 2N–O). Together, these data suggest that Nlrp3 inflammasome activity is necessary for embryonic HSPC formation.

Overexpression of active IL1β enhances embryonic HSPC expansion

Previously reported effects of exogenous IL1β on embryonic HSPC formation relied on *ex vivo* culture (Orelio et al., 2008, 2009). To assess functional impact *in vivo,* an Hsp70-inducible transcript encoding the fully processed, active form of zebrafish IL1β was engineered (Vojtech et al., 2012) (Fig. 3A). Induction of active IL1β (actIL1β; 32hpf) increased *runx1/cmyb* expression in the developing aorta at 36hpf (Fig. 3B–C), which was confirmed by *runx1* qPCR (Fig. 3D). Numbers of $Flk1^+cMyb^+$ HSPCs were likewise

increased by flow cytometry (Fig. 3E). Consistent with the induction of an inflammatory response, expression of known target genes were increased with actIL1β induction (Fig. 3F) (Cortes et al., 2016; North et al., 2009) and numbers of neutrophils in *Tg(mpx:gfp)* embryos (Renshaw et al., 2006) were elevated by flow cytometry (Fig. 3G). Importantly, actIL1β overexpression at 24hpf was sufficient to recover wildtype levels of *runx1* expression in *il1b* and *pycard* morphants by 36hpf (Fig. S3A–D), confirming that the active form bypasses a functional requirement for inflammasome assembly and Caspa activity. Finally, expression of *cmyb* was significantly increased in the kidney marrow at 120hpf with actIL1β overexpression, consistent with an acute expansion of the HSPC pool (Fig 3H–I).

HSPC production is enhanced by inflammasome activation

To determine whether pharmacologic inflammasome activation could be utilized to promote HSPC production through endogenous IL1β production, *runx1/cmyb* expression was assessed in embryos treated with established agonists of inflammasome assembly (Jo et al., 2016). Nigericin (0.1μM), which induces inflammasome action through alterations in intracellular potassium, increased *runx1/cmyb* expression in the dorsal aorta (Fig. 4A–B), and *runx1* levels by qPCR (Fig. 4C). Acute inflammasome stimulation with nigericin or an alternative agonist, alum crystals (alum, 20 μg/mL), which prompts activation through lysosomal perturbations (Hornung et al., 2008), increased numbers of phenotypic $Flk1^{+}cMyb^{+}$ HSPCs (Fig. 4D). IL1β target expression was also increased by qPCR following inflammasome stimulation (Fig. 4E). These effects are likely due to enhanced proliferation, as numbers of dividing cells in 30hpf *Tg(EF1a:mAG-zGem(1/100))*^{tw0410h} embryos (Sugiyama et al., 2009) as well as numbers of $Flk1^{+}EdU^{+}$ cells in the aortic floor at 36hpf were elevated in nigericin-treated embryos (Fig. 4F–H). Epistasis analyses with *il6* morpholinos (Lim et al., 2017) suggest that *il6* upregulation is at least partially required downstream of inflammasome action to promote *runx1/cmyb* expression (Fig. S4A–B). Furthermore, forced expression of a dominant negative IkB transgene, which suppresses *il1b* transcription (Espín-Palazón et al., 2014), prevented nigericin from increasing *cmyb* in the aorta of *Tg(hsp70l:GAL4;UAS:dnnfkbiaa)* embryos at 36hpf (Jeong et al., 2007), confirming the requirement for NFκB priming and subsequent IL1β signaling to boost numbers of HSPCs *in vivo* (Fig. S4C). Analyses of embryos at 120hpf revealed that inflammasome stimulation (24–120hpf) was correlated with increases in the proportion of $Rag2^{+}$ T lymphocytes (Langenau et al., 2003), Mpx^{+} neutrophils, and $Mfap4^{+}$ macrophages, while suppressing the frequency of $Gata1^{+}$ erythroblasts (Traver et al., 2003), consistent with recent reports (Tyrkalska et al., 2019) (Figure 4I; Fig. S4D–I). To determine whether there were lasting effects of embryonic inflammatory stimulation on adult steady-state hematopoiesis, lineage distribution was assessed in kidney marrow from inflammasome-stimulated embryos. This analysis revealed no significant alterations in lymphoid, myeloid, or precursor compartments at 3 months of age (Fig. S4J). Taken together, these data indicate that transient inflammasome activation expands developing HSPCs, which may temporarily restrict erythroid commitment of embryonic progenitors in favor of lympho-myeloid potential, without compromising adult HSPC differentiation capacity or maintenance.

Macrophages are an important source of IL1β during HSPC formation

Inflammasome activation is thought to occur primarily in myeloid cells. To investigate the cell-type(s) involved in inflammasome regulation of embryonic HSPC production, primitive myeloid populations, vasculature, and developing HSPCs were profiled for expression of inflammasome components. Consistent with prior analyses (Nguyen-Chi et al., 2014) and our observations for Il1β:EGFP expression (Fig. S1F–G), *il1b* was significantly enriched (225-fold) in Mpeg1^{+} macrophages (Palha et al., 2013) and Mpx^{+} neutrophils (128-fold) isolated by FACS compared with the bulk negative (Mpeg1^{-}Mpx^{-}) population at 48 hpf; *caspa* and *nlrp3* were also significantly enriched (10-fold) in macrophages (Fig. 5A). Inflammasome components were also detected at 48hpf in FACS-isolated Flk1^{+} vasculature and Flk1^{+}cMyb^{+} HSPCs, with significant enrichments in *nlrp3l* (Flk1^{+}) and *pycard/nlrp3* (Flk1^{+}cMyb^{+}) compared with the bulk negative (Flk1^{-}cMyb^{-}) fraction (Fig. 5B). Expression of *il1b* in FACS-isolated Flk1^{+} and Mpeg1^{+} populations from Tg(*mpeg1:gfp;flk1:mCherry*) embryos (Ellett et al., 2011) indicated the strongest response to metabolic stimulation prior to HSPC specification (12–24hpf) was in macrophages (Fig. S5A). Imaging of *Tg(pycard:pycard-EGFP)* embryos (Kuri et al., 2017) (30 hpf) revealed that many pycard^{bright} cells surrounding the aorta co-express the macrophage reporter *Tg*(*mpeg1:mCherry)* (Fig. 5C)(Ellett et al., 2011), together suggesting that macrophages serve as the major local source of inflammasome-processed IL1β during the onset of HSPC formation.

To determine whether the effects of inflammasome stimulation required myeloid cells, inflammasome activation was performed in embryos with or without knockdown of myeloid transcriptional regulators *spi1a/1b* (Bukrinsky et al., 2009). Morphant embryos exhibited a substantial reduction in macrophages, with a more modest effect on neutrophil number (Fig. S5B). As with prior studies, *spi1a/1b* morphants had reduced *runx1* expression (Li et al., 2014) (Fig. 5D; Fig. S5C). While overexpression of actIL1β partially recovered *runx1* expression in the aorta of *spi1a/1b* morphants at 36hpf, nigericin stimulation failed to expand HSPC numbers in morphant embryos at 72hpf (Fig. S5C–D, Fig. 5D–E). In further support of an essential role for macrophages, chemical ablation of macrophages to approximately 38% of untreated controls in *Tg(mpeg1:GAL4;UAS:nfsB-mCherry)* embryos (Palha et al., 2013) prevented an increase in *cmyb* expression in the CHT at 72hpf in response to inflammasome stimulation (Fig. 5F–G; Fig. S5E). Similarly, macrophage-specific blockade of NFκB activity, and thus inflammasome priming, in *Tg(mpeg:GAL4;UAS:nfsB-mCherry;UAS:dnikbaa)* embryos significantly impaired acquisition of *cmyb* expression in the CHT when compared to controls (Fig. 5H). Altogether, these data suggest that NFκB priming and inflammasome activation in macrophages positively influences HSPC number in the embryo.

IL1β signals are received by HSPCs to further prime inflammasome activity

To assess whether developing HSPCs in the embryonic dorsal aorta can directly respond to IL1β stimulation provided by accessory macrophages, expression of a predicted IL-1 receptor 1 ortholog, *il1rl1*, was profiled and found to be significantly enriched in Flk1^{+}cMyb^{+} HSPCs when compared with bulk vasculature and the non-endothelial fraction (Fig. 6A). Knockdown of *il1rl1* (Fig. S6A) significantly reduced *runx1/cmyb* expression (Fig. 6B–C)

and numbers of CD41$^+$ HSPCs (Fig. 6D), confirming a functional role. As IL1β signaling is known to induce NFκB activation and *il1b* transcription (Dinarello, 2009), this raises the possibility that inflammasome priming and activation could subsequently be propagated within Il1rl1$^+$ HSPCs. In support of this concept, CD41$^+$ HSPCs were found to upregulate *il1b* at 48hpf in response to glucose treatment initiated at 12hpf (Fig. 6E). Furthermore, driving *actil1b* expression in Flk1$^+$ cells was also sufficient to increase *runx1* expression by WISH (Fig. S6B–C). Finally, in agreement with the observed enrichment of *pycard* by qPCR in Flk1$^+$cMyb$^+$ HSPCs (Fig. 5B), time-lapse microscopy confirmed the presence of budding Pycard$^+$Flk1$^+$ cells in the aorta (Fig. 6F, Movie S1, 34–36hpf), suggesting that developing HSPCs acquire competence to undergo inflammasome activation during the EHT process. Taken together, these data indicate that while macrophages provide critical inductive IL1β signals to promote embryonic HSPC development, this signal may be further relayed within nascent HSPCs to amplify their number (Fig. 6G).

Inflammasome stimulation promotes human HSPC expansion

To build on the observations that inflammasome activity expands developing zebrafish HSPCs, a possible role for inflammasome stimulation in regulating human HSPC production from iPSC-derived CD34$^+$ hemogenic endothelial cell cultures was next explored (Ditadi et al., 2015) (Fig. 7A). On day 2 post CD34 enrichment, cultures poised to undergo endothelial-to-hematopoietic transition (EHT) expressed *IL1R*, as well as NLRP3 inflammasome components (Gupta et al., 2019; Son et al., 2015; Spandidos et al., 2010), indicating that cells were competent to receive IL1β and further activate the inflammasome (Fig. 7B). Given the absence of CD34$^-$CD45$^+$ cells in EHT cultures on day 2 post CD34-enrichment (Fig. S7A), we postulated that addition of macrophages might be necessary to enhance the efficiency of IL1β production and inflammasome stimulation *in vitro*. To this end, THP-1 human monocytes were primed with lipopolysaccharide (LPS) to induce *IL1B* (Chanput et al., 2014; Sharif et al., 2007), seeded in transwell inserts over developing CD34$^+$ EHT cultures, and subsequently activated with nigericin on day 2 of culture (Fig. S7B). Intriguingly, nigericin stimulation of co-cultures exerted a significant effect on phenotypic HSPC number (Fig. S7C). Co-culture with unstimulated or LPS-primed monocytes alone also improved the frequency of CD34$^+$CD45$^+$ phenotypic HSPCs over untreated controls, in the absence of nigericin-mediated inflammasome activation, suggesting that the monocytes supply both inflammasome-dependent and independent supportive factors to the HSPCs. As inflammasome stimulation with nigericin alone also significantly increased the frequency of CD34$^+$/CD45$^+$ cells in the absence of monocytes, we sought to further clarify the impact of inflammasome stimulation in the absence of other confounding paracrine signals.

As our zebrafish studies suggested that developing HSPCs are competent to not only respond to IL1β, but later activate the inflammasome, the impact of direct nigericin stimulation was further assessed. In addition to increasing the proportion of CD34$^+$CD45$^+$ phenotypic hematopoietic progenitor cells assayed on day 7 in a dose-dependent manner, nigericin treatment of EHT cultures also elevated the expression of *RUNX1c* within this population (Challen and Goodell, 2010; Navarro-Montero et al., 2017) (Fig. 7C–D), suggestive of improved commitment and/or expansion. Importantly, inflammasome stimulation increased the total numbers of functional hematopoietic colony-forming units as

well as the number of CFU-GEMM colonies harvested on day 7 of EHT cultures (Fig. 7E). To determine whether inflammasome stimulation improved *in vivo* engraftment and differentiation capacity of iPSC-derived HSPCs, transplantation studies were performed. While transient inflammasome stimulation showed a trend toward enhancing human $CD45^+$ engraftment of transplanted mice after 8 weeks, the overall lack of robust engraftment in the absence of additional genetic modification made it difficult to discern a selective advantage in multi-potent repopulating potential (Fig. 7F; Fig. S7D). Intriguingly, consistent with *in vivo* observations in the zebrafish embryo, continued differentiation in suspension cultures demonstrated that nigericin stimulation induced a strong bias toward myeloid over erythroid fate (Fig. 7G; Fig. S7E–F). Importantly, however, inflammasome-expanded progenitors were equally able to undergo lymphoid commitment *in vitro*, resulting in a net increase in iPSC-derived $CD5^+CD7^+$ pro-T cell formation (Fig. 7H; Fig. S7G). Together, these data indicate that inflammasome activation promotes short-term expansion of human HSPCs, and restrains premature erythroid differentiation *in vitro.*

Discussion

In the vertebrate embryo, there is emerging evidence that sterile inflammation is an endogenous regulator of HSPC number and lineage output. However, it has remained unclear how these signals are initiated and relayed to regulate the specification and differentiation of HSPCs. Here, we show that metabolic alterations associated with embryonic growth trigger the production of inflammatory signals through activation of the NLRP3 inflammasome to expand HSPC number. Our time course analyses demonstrate a precise temporal correlation between the peak of glucose bioavailability and the onset of HSPC budding from the aortic floor (Kissa and Herbomel, 2010). This energy-intensive budding process is also contemporaneous with the ability of embryos to utilize oxidative phosphorylation, which results in accumulation of ROS, a known NLRP3 inflammasome agonist, and HIF1α stabilization, which promotes *il1b* transcription in the embryo (Harris et al., 2013; Guo et al., 2015; Jo et al., 2016; Ogryzko et al., 2019). Coincidentally, global expression of inflammasome components increased during the time of HSPC formation, while *il1b* was observed to accumulate in developing myeloid populations by qPCR and in aortic endothelium of *Tg(il1b:EGFP)* embryos. Exogenous glucose stimulation further induced *il1b* expression, consistent with established connections between heightened metabolism and ROS formation in macrophages and subsequent IL1β production (Tannahill et al., 2013; Hall et al., 2018). Importantly, our observations that the endogenous peak of embryonic glucose concentration subsides after HSPC formation also suggests that the metabolic inflammasome stimulation is likely transient in nature, minimizing the potential for HSPC exhaustion and/or damage. Together, our data indicate that dynamic developmental fluctuations of energy sources coordinate the timing of sterile inflammatory signaling and the subsequent production of embryonic HSPCs, which may be suboptimal in current *in vitro* culture approaches.

IL1β was previously reported to impact murine HSPC formation (Orelio et al., 2008, 2009), however, its upstream developmental regulator was not fully defined. Consistent with a role for the NLRP3 inflammasome in regulating sterile IL1β activity in adult mammals (Haneklaus and O'Neill, 2015), morphants and mutants of zebrafish NLRP3 inflammasome

components demonstrated a reduction in robust HSPC formation. These data reveal a previously undescribed role for NLRP3 activity as a homeostatic regulator of developmental hematopoiesis. Furthermore, epistasis analyses suggest that energy metabolism promotes inflammasome activity to increase IL1β production and HSPC marker expression. Our data also indicate that NFκB activity is a key requirement for inflammasome-mediated regulation of HSPC number *in vivo*, and is required in macrophages to initiate normal levels of *cmyb* expression. Intriguingly, NFκB also regulates Notch signaling within hemogenic endothelium (Espín-Palazón et al., 2014; He et al., 2015), and can regulate Hif1α, which was previously shown by our laboratory to promote HSPC development (Tirziu et al., 2012; D'Ignazio et al., 2016; Harris et al., 2013). Given that IkB itself is also an NFκB target (Sun et al., 1993), it will be interesting to further dissect how these transcriptional networks converge to establish and subsequently modulate inflammatory activity during HSPC formation. Although prior *in vitro* work has indicated that inflammasome priming is necessary to boost NLRP3 expression to induce robust pro-IL1β cleavage in macrophages (He et al., 2016), we find that human iPSC-derived $CD34^+$ cultures basally express low levels of inflammasome components and respond to low concentrations of nigericin. Thus, it is possible that combinatorial use of agonists to further prime or stimulate the inflammasome may elicit a potent impact on HSPC production.

Our studies support the concept that macrophages are a major source of IL1β and play an important role in initiating inflammasome activation during zebrafish HSPC formation. Based on our *in vivo* time-lapse imaging data and inflammasome expression profiling, we propose that macrophage-derived IL1β might propagate inflammasome activity within $Il1rl1^+$ HSPCs through downstream NFκB activation (Bauernfeind et al., 2009; Dinarello, 2009). Recent transcriptome analyses of aortic-associated macrophages from the mouse embryo similarly indicate expression of a multitude of cytokines and growth factors which may support HSPC production, including inflammasome-derived IL18 and IL1β (Mariani et al., 2019), both of which result in downstream NFκB activity and can generate similar cellular responses (Dinarello, 1999). Although not specifically enriched in murine $CD206^+$ macrophages, regulation of IL1β at the protein level suggests that IL1β is likely an influential paracrine signal (Orelio et al., 2008). However, our data do not diminish the possibility that other macrophage-derived factors, or additional cell populations, including neutrophils, can "prime" inflammasome activation or cooperate with downstream IL1β signaling to further promote HSPC expansion. Intriguingly, macrophages are rare in human EHT cultures during the window of inflammasome stimulation; addition of monocytes alone positively influenced the frequency of $CD34^+CD45^+$ phenotypic HSPCs formed in human EHT cultures. Thus, absence of these additional cues from iPSC cultures might explain the suboptimal numbers of HSPCs generated with multipotent engraftment activity to date. In future work, it will be of interest to evaluate whether the presence of ontogenically distinct myeloid populations differentially influence developing human EHT cultures *in vitro*, and the precise temporal windows needed for their interaction, to maximize HSPC production and maintenance.

Finally, our findings indicate that inflammasome activation appears to robustly expand the HSPC pool *in vivo* and *in vitro*. A frequent concern with stimulation of proliferative expansion in HSPCs is the potential for exhaustion or premature differentiation (Mirantes et

al., 2014). While we found no evidence for exhaustion *in vivo*, a reduction in erythroid differentiation was observed, suggesting that inflammasome activation may also restrain erythroid commitment within HSPCs. This would effectively counter the effects of embryonic hypoxia, which strongly induces erythroid differentiation signals in the embryo (Imtiyaz and Simon, 2010). In support of this idea, a recent report demonstrates that embryonic HSPCs cell-autonomously activate low levels of Caspase-1 to inactivate Gata1 and prevent erythroid differentiation in favor of myeloid differentiation (Tyrkalska et al., 2019). Although our data also indicate a reduction in erythroid differentiation in the context of inflammasome activity, this may be a secondary signaling mechanism that is initiated after macrophage-derived IL1β drives HSPC expansion. This latter hypothesis is supported by our observation that similar proportions of human erythroid colonies and lymphoid cells are formed from inflammasome-stimulated progenitors *in vitro*. Conversely, when HSPCs are left to differentiate in nigericin-treated suspension cultures, or when zebrafish embryos undergo prolonged inflammasome stimulation, both eventually exhibit lineage bias toward lymphoid and myeloid fates, mimicking inflammation-associated anemia. This effect may be due to amplified production of downstream cytokines, including IL6 (Nemeth et al., 2004; Zhao et al., 2014). These findings also underscore the importance of the timing and duration of inflammasome action in providing the optimal HSPC amplification response *in vitro*, and may be one reason why a prior study reported no benefit of exogenous inflammatory cytokines on the numbers of phenotypic human HSPCs specified *in vitro* (Giorgetti et al., 2017). It is likely that the acute stimulation of inflammasome activation in our cultures provides a more physiological inflammatory signaling cascade to better support HSPC expansion, as opposed to a continuous supply of recombinant cytokines, which may damage self-renewal and/or differentiation potential. As such, we favor a model in which endogenous, acute IL1β production serves to primarily expand multipotent HSPCs and secondarily restrain erythroid potential *in vitro* and *in vivo*.

Together, these studies reveal that inflammasome activation serves as a developmental metabolic sensor to trigger IL1β production and expand developing HSPCs. In addition, transient inflammasome activation *in vitro* provides a physiological burst of IL1β that expands functional human HSPCs. Inflammasome activity is initiated by macrophages *in vivo*, which, alongside other work, highlights the importance of supporting cell types in the development and function of HSPCs. It will be of interest to further explore and optimize potential co-culture conditions of human hemogenic endothelium alongside myeloid populations to better recapitulate the metabolic cues they interpret and relay to developing HSPCs to promote their expansion and maintenance.

STAR METHODS

RESOURCE AVAILABILITY

Lead Contact—Requests for resources should be directed to and will be fulfilled by the lead contact, Trista E. North (Trista.north@childrens.harvard.edu).

Materials Availability—Materials generated in this study are available upon request.

Data and Code Availability—This study did not generate datasets or code requiring public database deposition.

EXPERIMENTAL MODEL AND SUBJECT DETAILS

Zebrafish—Zebrafish maintenance and experiments were performed according to guidelines set forth by the Beth Israel Deaconess Medical Center and Boston Children's Hospital Institutional Animal Care and Use Committees. Adult zebrafish were housed in a standard circulating water system at 27°C and fed a brine shrimp diet. AB or TU strains were used for wild-type studies and outcrosses. Transgenic and mutant lines are noted in the Key Resources Table. Mutants were genotyped by PCR followed by Sanger sequencing. Transgenics were identified by fluorescence microscopy or transgene expression by WISH. For embryonic studies, males and females were separated off-system overnight, and barriers removed the following morning to allow for timed embryo generation. After collection, embryos were maintained under static conditions in E3 embryo buffer in incubators at 28.2°C, 25°C, or 22°C to desired developmental stages reported in figure legends. Embryos exhibiting developmental abnormalities or delay were discarded. Sex is not determined in zebrafish embryos and therefore was not assessed. For adult kidney marrow analyses, male zebrafish were maintained at equivalent tank densities until the experimental endpoint (3 months).

Mice—Murine housing, maintenance, and transplantation studies were performed in accordance with guidelines set forth by the Boston Children's Hospital Institutional Animal Care and Use Committee. Female NBSGW (NOD.Cg-*Kit*$^{W-41J}$ *Tyr* $^{+}$ *Prkdc*^{scid} *Il2rg*^{tm1Wjl}/ThomJ) immunocompromised mice were purchased from Jackson Laboratory and maintained in a standard barrier facility. 8–12 week old mice were used for transplantation. Antibiotic water (0.5mg/mL Sulfatrim) was given for 2 weeks post-transplant.

Primary Cells—Irradiated murine embryonic fibroblasts (MEF; mixed/unknown sex) used to passage iPSCs were purchased directly from ThermoFisher Scientific. Human umbilical cord blood mononuclear cells isolated from unknown donors were purchased (Stem Cell Technologies) and used for gating controls in transplantation analyses.

Cell lines—1157.2-iPS cells were generated by the Boston Children's Hospital hESC (human embryonic stem cell) Core Facility from a healthy male donor under Institutional Review Board approved protocols. iPSCs were maintained on hESC-qualified Matrigel-coated dishes in Stemflex medium (ThermoFisher Scientific) at 37°C /20% O_2/5% CO_2 and routinely karyotyped and tested for mycoplasma contamination. THP-1 monocytes (from a male with monocytic leukemia (Tsuchiya et al., 1980)) were purchased for use (Invivogen) and maintained in RPMI medium with 2mM glutamine, 25mM HEPES, and 10% fetal bovine serum (FBS) at 37°C /20% O_2/5% CO_2. Authenticity, purity and functionality to activate the inflammasome was verified by the vendor.

Human iPSC differentiation—1157.2-iPSCs were differentiated into hemogenic endothelium essentially as described (Sugimura et al., 2017). In brief, iPSCs were cultured for one passage on CF-1 irradiated MEFs prior to embryoid body (EB) formation. Colonies

were detached using Collagenase IV and seeded into low attachment dishes (Corning) in aggregation media (Sturgeon et al., 2014). 24 hours later bFGF (5 ng/ml) was added. On day 2 aggregation media was supplemented with bFGF (5 ng/ml), BMP4 (10 ng/ml), CHIR99021 (3 μM) and SB431542 (6 μM). For the following 3 days, EB media (Stempro-34, Thermo Fisher Scientific) was supplemented with ascorbic acid (1 mM), holo-Transferrin (150 μg/ml) and α-Monothioglycerol (MTG, 0.4 mM)). On day 6 EB media was supplemented with bFGF (5 ng/ml), VEGF (15 ng/ml), IL-6 (10 ng/ml), IL-11 (5 ng/ml), IGF-1 (25 ng/ml), SCF (50 ng/ml) and EPO (2U/ml). EBs were harvested on day 8 and dissociated with trypsin/EDTA followed by collagenase IV. $CD34^+$ hemogenic endothelium was enriched by Magnetic-activated cell sorting (MACS) (Miltenyi). For MACS, freshly dissociated EBs were filtered through a 40 μm cell strainer and incubated with anti-CD34 magnetic beads for 30 min on ice per the manufacturer's recommendation. Unbound beads were washed off with Phosphate Buffered Saline (PBS)/2%FBS and cells separated using LS columns. $CD34^+$ cells were counted and 50k cells per well of a 24 well plate were plated onto Matrigel (ThermoFisher Scientific) coated dishes in EHT media (EB media + BMP4 (10 ng/ml), bFGF (5 ng/ml), IL-3 (30 ng/ml), IL-6 (10 ng/ml), IL-11 (5 ng/ml), IGF-1 (25 ng/ml), VEGF (5 ng/ml), SCF (100 ng/ml), EPO (2U/ml), TPO (30 ng/ml), FLT-3L (10 ng/ml), SHH (20 ng/ml), Angiotensin II (10 μg/ml), Losartan (100 μM). Nigericin (1–10 nM) or EtOH treatment (for controls) was performed on day 2 prior to emergence of round floating cells. Once EB differentiation was started, cultures were incubated at 37°C in a 5% CO_2/5%O_2/90% N_2 environment.

METHOD DETAILS

Generation of inducible IL1β transgenic zebrafish

The *Tg(hsp70l:il1b)* line was generated by PCR amplification of the portion of *il1b* transcript corresponding to amino acids 104–272 (following the Caspa cleavage site) (Vojtech et al., 2012), insertion into a Gateway middle entry vector (pME-MCS), and subsequent multi-site Gateway recombination (Invitrogen) into a destination vector carrying the *cryaa:cerulean* transgene using the Tol2Kit workflow (plasmids listed in Key Resources Table) (Kwan et al., 2007). Germline transgenesis was achieved in 7 founders via co-injection of the construct with Tol2 transposase mRNA. Overexpression of *il1b* was confirmed in embryos by WISH after incubation at 38°C for 30 minutes. For endothelial-specific induction of active *il1b,* a p5E-flk1 promoter construct (Addgene) was utilized in place of the Hsp70l promoter construct, and chimeric injected embryos were screened for expression of *cryaa:cerulean* by WISH alongside *runx1* and *il1b.*

Zebrafish embryo injections

Morpholinos (Gene Tools) were loaded into a needle pulled from 1.0mm borosilicate glass capillary tubes, and injected into the yolk of fertilized eggs immobilized in agarose molds at the 1-cell stage using a microinjector (Narishige). Morpholinos are listed in Table S1. For transgenesis, constructs were injected directly into the fertilized egg cell.

Zebrafish Chemical Exposures and WISH

Groups of 20 stage-matched embryos were arranged in 6 well plates in 5mL E3 water with or without chemical treatments of interest. Embryos were manually dechorionated and fixed in 4% paraformaldehyde for WISH analyses. Pigment was subsequently removed with 0.8%KOH/0.9%H_2O_2 treatment; embryos were then dehydrated into 100% methanol prior to WISH using standard published protocols and probes (http://zfin.org/ZFIN/Methods/ThisseProtocol.html). Briefly, embryos were permeabilized with 10μg/mL Proteinase K (Millipore Sigma), re-fixed in 4% paraformaldehyde, washed in 1xPBS containing 0.1% Tween (PBST) and hybridized with digoxigenin-UTP-labeled riboprobes in hybridization buffer containing 50% formamide at 70°C overnight. Embryos were washed in sodium citrate buffer/0.1% Tween and incubated overnight with a digoxigenin antibody conjugated to alkaline phosphatase in PBST. After several PBST washes, antibody staining was revealed by incubation in Tris buffer (pH 9.5) with BCIP/NBT substrate (Millipore Sigma). Stained embryos were directly compared with stage-matched sibling controls across multiple clutches, with the exception of mutant clutches, which were compared alongside matched wild-type or heterozygote clutches as indicated. The intensity of expression was qualitatively categorized by high (abbreviated hi), medium (med), or low (lo), relative to the median intensity of the control group for a given clutch. For *runx1/cmyb* expression at 36hpf, a score of “hi” typically reflects continuous aortic signal with robust thickness, indicating numerous cell clusters, “medium” denotes modest, yet continuous aortic signal, and low signal indicates spotty/discontinuous aortic signal. At least 25 embryos from a minimum of two independent clutches were analyzed per treatment condition and/or genotype, with phenotype scoring independently confirmed. WISH images were captured on a Zeiss Axio Imager A1 equipped with Axio Vision software; images were selected to represent the median expression level for each treatment/condition. Area of stained kidney marrows were quantified in images using Fiji software (Schindelin et al., 2012).

EdU labeling and fluorescence microscopy

Embryos were exposed to 500μM EdU in E3 water (10% DMSO final) for 1 hour at 4°C. Embryos were fixed in 4% paraformaldehyde, permeabilized with 1% Triton for 1 hour, and labeled with Alexa Fluor 647 using the Click-iT reaction (Thermo Fisher Scientific) for 1 hour at room temperature according to the manufacturer’s instructions. Embryos were mounted in 3% methylcellulose and captured on a Zeiss LSM880 Inverted Confocal Microscope. Live *Tg(pycard:pycard-EGFP)* and *Tg(il1b:EGFP)* embryos were mounted in 1.5% low melting agarose and imaged on a Zeiss LSM880 Inverted Confocal Microscope or a Nikon Ti2 inverted microscope equipped with a CSU-W1 spinning disk confocal unit and iXon888 life camera. *Tg(CD41:EGFP)* and *Tg(EF1a:mAG-zGem(1/100))*^{rw0410h} live embryos were imaged on a Zeiss Discovery V8 (Axio Vision software). Cell counts were performed manually in Fiji software. Image brightness and contrast were adjusted in Fiji or Powerpoint.

Glucose measurement assay

Embryos from two independent clutches were reared at 28.2°C and treated at 24hpf with phenylthiourea (0.003%) to prevent pigmentation. Groups of 24 embryos were then

dechorionated at specified timepoints and flash frozen in 1xPBS on dry ice. Samples were homogenized and spun down to remove excess debris; supernatants were stored at −80°C. Supernatants were incubated with substrate from an Amplex Red Glucose measurement kit and glucose measurements were obtained from absorbance readings according to the manufacturer's instructions (Fisher Scientific).

Flow cytometry

Pools of zebrafish embryos/larvae were dechorionated and resuspended in 500μL Liberase TM (Millipore Sigma) solution (75μg/mL in 1xPBS/1mM EDTA), incubated at 34°C and dissociated with a 1000μL pipette every 20–30 minutes until embryo trunks are no longer visible (Frame et al., 2017); each data point represents 4 or 5 zebrafish. Adult male kidney marrow was manually triturated in 1xPBS/1mM EDTA with a 1000μL pipette. Zebrafish samples were passed through a 30μm filter, washed in PBS, and labeled with Sytox Red (Invitrogen) to 5nM prior to analysis. Human cells were blocked with TruStain FcX and labeled with antibodies (listed in the Key Resources Table) at room temperature for 20 minutes, followed by DAPI addition (to 0.5μg/mL final) to exclude dead cells. Flow cytometric data were collected on a FACSCanto, LSRII, or LSRFortessa (BD) and cell sorting was performed on a FACSAria II (BD). Data were analyzed using FlowJo X (BD). $CD41^{+}$ zebrafish HSPCs were gated separately from the $CD41^{hi}$ thrombocyte population (Lin et al., 2005; Ma et al., 2011).

RNA isolation and quantitative PCR

Total zebrafish embryo RNA was isolated from pools of >20 embryos using the RNAqueous kit according to the manufacturer's protocol (Invitrogen). Briefly, embryos were mechanically homogenized in the lysis buffer and treated with DNAse I (Invitrogen) after elution from the column. For sorted zebrafish myeloid cell and $CD41^{+}$ populations, RNA was isolated using an RNEasy Micro kit (Qiagen) and DNAse was applied directly on the column per the manufacturer's protocol. cDNA was synthesized using Superscript III Supermix or Superscript VILO cDNA Synthesis kit (Invitrogen). $Flk1^{+}$/$cMyb^{+}$ sorted cell cDNAs were prepared using the NuGEN Ovation RNA Amplification System V2 according to the manufacturer's protocol (Cortes et al., 2016; Lim et al., 2017). RNA was isolated from iPSC-derived populations using the RNEasy Micro kit Plus (Qiagen) and cDNA was transcribed using the Maxima Reverse Transcriptase kit (Thermo Fisher Scientific). Quantitative PCR was performed on a CFX384 (BioRad) or ABI7900 (Applied Biosystems) using either SYBR green Master mix or Taqman universal master mix (Applied Biosystems). Absolute expression level in each sample was calculated relative to reference genes (*eef1a1l1* for Taqman assays; and *b-actin, 18s,* or *GAPDH* for SYBR green) (Esain et al., 2015) using the Delta/delta Ct Method or the PCR Miner interface (Zhao and Fernald, 2005), fold change was calculated relative to the negative control or untreated sample population within each biological clutch or group of clutches. For sorted cell populations, fold change was calculated relative to the bulk negative control fraction. Primer sequences are listed in Table S1.

Hematopoietic colony assay

Hematopoietic colony potential of the live floating cells (4.25k-15k) on day 7 of EHT culture was assessed in methylcellulose cultures (MethoCult™ SF H4636; StemCell Technologies). Dishes were kept in a humidified chamber in the incubator for 14 days, then scored manually and blindly.

Monocyte co-cultures

Human THP-1 monocytes (Invivogen) were pre-stimulated with LPS (1 μg/ml) overnight according to the manufacturer's instructions. The following day, 25K THP-1 cells were seeded in the upper well of transwell inserts (0.4μm pore size, Corning); while 50K iPSC-derived $CD34^+$ MACS-purified hemogenic endothelial cells were seeded on the bottom 2 days prior in EHT medium. Nigericin (10 nM) was subsequently added to the EHT co-culture.

T cell differentiation

Human iPSCs were differentiated to form embryonic bodies, and $CD34^+$ hemogenic endothelium was enriched from dissociated day 8 EBs as above. $CD34^+$ cells were plated under T lymphoid differentiation conditions using the StemSpan T cell generation kit (#09940, Stem Cell Technologies) according to the manufacturer's instructions. Nigericin (10 nM) or EtOH (for controls) was added on day 2, and $CD45^+CD5^+CD7^+$ pro-T cells were detected after 2 weeks.

Transplantation

Human iPSC-derived hematopoietic progenitors were transplanted intrafemorally into 8–12 week old female immunodeficient NOD.Cg-*Kit*$^{W-41J}$ *Tyr* $^+$ *Prkdc*^{scid} *Il2rg*^{tm1Wjl}/ThomJ (NBSGW) mice in the absence of irradiation. After 8 weeks, femoral bone marrow was harvested using a mortar and pestle and analyzed by flow cytometry.

QUANTIFICATION AND STATISTICAL ANALYSIS

Data analyses were performed using GraphPad Prism. Error bars indicate SD unless otherwise indicated; statistical significance was determined by two-tailed Student's T-test unless otherwise indicated. In some cases, differences in cell number, frequency, or expression were normalized to the average control value within clutches, or to the average control well in iPSC differentiation assays. Significance of WISH phenotype distributions was determined by Chi-square analysis.

Supplementary Material

Refer to Web version on PubMed Central for supplementary material.

Acknowledgments

We thank the Boston Children's Hospital flow cytometry core, Yi Zhou for genomic expertise, Mohamad Najia for flow cytometry help, Wade Sugden for cloning expertise, Maria Leptin for *pycard:EGFP* line and *caspa* mutants, David Tobin for *pycard* mutants, David Traver for the *UAS:dnikbaa* line, and Leonard Zon for *mpeg:NTR-mCherry* and *flk1:mCherry* lines. Work was funded by the National Institutes of Health: T32 HL007893 (JMF), R01

DK098241 (TEN), R01 HL152636 (TEN), R24 DK092760 (GQD/TEN), U01 HL134812 (GQD/TEN), and the German Research Foundation (CK). Graphical abstract created from Biorender.com.

Declaration of Interests

GQD holds equity in 28/7 Therapeutics and Epizyme, has received sponsored research support from Megakaryon, and holds patents pertaining to HSPC production from iPSCs.

References

Abderrazak A, Syrovets T, Couchie D, El Hadri K, Friguet B, Simmet T, and Rouis M (2015). NLRP3 inflammasome: From a danger signal sensor to a regulatory node of oxidative stress and inflammatory diseases. Redox Biol. 4, 296–307. [PubMed: 25625584]

Baldridge MT, King KY, Boles NC, Weksberg DC, and Goodell MA (2010). Quiescent haematopoietic stem cells are activated by IFN-gamma in response to chronic infection. Nature 465, 793–797. [PubMed: 20535209]

Bauernfeind FG, Horvath G, Stutz A, Alnemri ES, MacDonald K, Speert D, Fernandes-Alnemri T, Wu J, Monks BG, Fitzgerald KA, et al. (2009). Cutting edge: NF-kappaB activating pattern recognition and cytokine receptors license NLRP3 inflammasome activation by regulating NLRP3 expression. J. Immunol. Baltim. Md 1950 183, 787–791.

Bertrand JY, Kim AD, Violette EP, Stachura DL, Cisson JL, and Traver D (2007). Definitive hematopoiesis initiates through a committed erythromyeloid progenitor in the zebrafish embryo. Development 134, 4147–4156. [PubMed: 17959717]

Bertrand JY, Chi NC, Santoso B, Teng S, Stainier DYR, and Traver D (2010). Haematopoietic stem cells derive directly from aortic endothelium during development. Nature 464, 108–111. [PubMed: 20154733]

Böiers C, Carrelha J, Lutteropp M, Luc S, Green JCA, Azzoni E, Woll PS, Mead AJ, Hultquist A, Swiers G, et al. (2013). Lymphomyeloid Contribution of an Immune-Restricted Progenitor Emerging Prior to Definitive Hematopoietic Stem Cells. Cell Stem Cell 13, 535–548. [PubMed: 24054998]

Bukrinsky A, Griffin KJP, Zhao Y, Lin S, and Banerjee U (2009). Essential role of spi-1-like (spi-1l) in zebrafish myeloid cell differentiation. Blood 113, 2038–2046. [PubMed: 19131555]

Camell C, Goldberg E, and Dixit VD (2015). Regulation of Nlrp3 inflammasome by dietary metabolites. Semin. Immunol 27, 334–342. [PubMed: 26776831]

Challen GA, and Goodell MA (2010). Runx1 isoforms show differential expression patterns during hematopoietic development but have similar functional effects in adult hematopoietic stem cells. Exp. Hematol 38, 403–416. [PubMed: 20206228]

Chanput W, Mes JJ, and Wichers HJ (2014). THP-1 cell line: An in vitro cell model for immune modulation approach. Int. Immunopharmacol 23, 37–45. [PubMed: 25130606]

Clements WK, and Traver D (2013). Signalling pathways that control vertebrate haematopoietic stem cell specification. Nat Rev Immunol 13, 336–348. [PubMed: 23618830]

Cortes M, Chen MJ, Stachura DL, Liu SY, Kwan W, Wright F, Vo LT, Theodore LN, Esain V, Frost IM, et al. (2016). Developmental Vitamin D Availability Impacts Hematopoietic Stem Cell Production. Cell Rep. 17, 458–468. [PubMed: 27705794]

Daniel MG, Pereira C-F, Lemischka IR, and Moore KA (2016). Making a Hematopoietic Stem Cell. Trends Cell Biol. 26, 202–214. [PubMed: 26526106]

Dhillon SS, Torell F, Donten M, Lundstedt-Enkel K, Bennett K, Rännar S, Trygg J, and Lundstedt T (2019). Metabolic profiling of zebrafish embryo development from blastula period to early larval stages. PLOS ONE 14, e0213661. [PubMed: 31086370]

D'Ignazio L, Bandarra D, and Rocha S (2016). NF–κB and HIF crosstalk in immune responses. Febs J. 283, 413–424. [PubMed: 26513405]

Dinarello CA (1999). IL-18: A TH1 -inducing, proinflammatory cytokine and new member of the IL-1 family. J. Allergy Clin. Immunol 103, 11–24. [PubMed: 9893178]

Dinarello CA (2009). Immunological and Inflammatory Functions of the Interleukin-1 Family. Annu. Rev. Immunol 27, 519–550. [PubMed: 19302047]

Dinarello CA (2011). A clinical perspective of IL-1β as the gatekeeper of inflammation. Eur. J. Immunol 41, 1203–1217. [PubMed: 21523780]

Ditadi A, Sturgeon CM, Tober J, Awong G, Kennedy M, Yzaguirre AD, Azzola L, Ng ES, Stanley EG, French DL, et al. (2015). Human definitive haemogenic endothelium and arterial vascular endothelium represent distinct lineages. Nat. Cell Biol 17, 580–591. [PubMed: 25915127]

Dror E, Dalmas E, Meier DT, Wueest S, Thévenet J, Thienel C, Timper K, Nordmann TM, Traub S, Schulze F, et al. (2017). Postprandial macrophage-derived IL-1β stimulates insulin, and both synergistically promote glucose disposal and inflammation. Nat. Immunol 18, 283–292. [PubMed: 28092375]

Duewell P, Kono H, Rayner KJ, Sirois CM, Vladimer G, Bauernfeind FG, Abela GS, Franchi L, Nuñez G, Schnurr M, et al. (2010). NLRP3 inflamasomes are required for atherogenesis and activated by cholesterol crystals that form early in disease. Nature 464, 1357–1361. [PubMed: 20428172]

Dzierzak E, and Speck NA (2008). Of lineage and legacy: the development of mammalian hematopoietic stem cells. Nat Immunol 9, 129–136. [PubMed: 18204427]

Ellett F, Pase L, Hayman JW, Andrianopoulos A, and Lieschke GJ (2011). mpeg1 promoter transgenes direct macrophage-lineage expression in zebrafish. Blood 117, e49–56. [PubMed: 21084707]

Esain V, Kwan W, Carroll KJ, Cortes M, Liu SY, Frechette GM, Sheward LMV, Nissim S, Goessling W, and North TE (2015). Cannabinoid Receptor-2 Regulates Embryonic Hematopoietic Stem Cell Development via Prostaglandin E2 and P-Selectin Activity: CNR2 Impacts Embryonic HSC Development. STEM CELLS 33, 2596–2612. [PubMed: 25931248]

Espín-Palazón R, Stachura DL, Campbell CA, García-Moreno D, Del Cid N, Kim AD, Candel S, Meseguer J, Mulero V, and Traver D (2014). Proinflammatory Signaling Regulates Hematopoietic Stem Cell Emergence. Cell 159, 1070–1085. [PubMed: 25416946]

Esplin BL, Shimazu T, Welner RS, Garrett KP, Nie L, Zhang Q, Humphrey MB, Yang Q, Borghesi LA, and Kincade PW (2011). Chronic Exposure to a TLR Ligand Injures Hematopoietic Stem Cells. J. Immunol 186, 5367–5375. [PubMed: 21441445]

Essers MAG, Offner S, Blanco-Bose WE, Waibler Z, Kalinke U, Duchosal MA, and Trumpp A (2009). IFNα activates dormant haematopoietic stem cells in vivo. Nature 458, 904–908. [PubMed: 19212321]

Frame JM, Lim S-E, and North TE (2017). Hematopoietic stem cell development: Using the zebrafish to identify extrinsic and intrinsic mechanisms regulating hematopoiesis. Methods Cell Biol. 138, 165–192. [PubMed: 28129843]

Giorgetti A, Castaño J, Bueno C, Díaz de la Guardia R, Delgado M, Bigas A, Espinosa L, and Menendez P (2017). Proinflammatory signals are insufficient to drive definitive hematopoietic specification of human HSCs in vitro. Exp. Hematol 45, 85–93.e2. [PubMed: 27693385]

Guo H, Callaway JB, and Ting JP-Y (2015). Inflammasomes: mechanism of action, role in disease, and therapeutics. Nat. Med 21, 677–687. [PubMed: 26121197]

Gupta G, Santana AKM, Gomes CM, Turatti A, Milanezi CM, Bueno Filho R, Fuzo C, Almeida RP, Carregaro V, Roselino AM, et al. (2019). Inflammasome gene expression is associated with immunopathology in human localized cutaneous leishmaniasis. Cell. Immunol 341, 103920. [PubMed: 31078283]

Hall CJ, Sanderson LE, Lawrence LM, Pool B, Kroef M.van der, Ashimbayeva E, Britto D, Harper JL, Lieschke GJ, Astin JW, et al. (2018). Blocking fatty acid–fueled mROS production within macrophages alleviates acute gouty inflammation. J. Clin. Invest 128, 1752–1771. [PubMed: 29584621]

Haneklaus M, and O'Neill LAJ (2015). NLRP3 at the interface of metabolism and inflammation. Immunol. Rev 265, 53–62. [PubMed: 25879283]

Harris JM, Esain V, Frechette GM, Harris LJ, Cox AG, Cortes M, Garnaas MK, Carroll KJ, Cutting CC, Khan T, et al. (2013). Glucose metabolism impacts the spatiotemporal onset and magnitude of HSC induction in vivo. Blood 121, 2483–2493. [PubMed: 23341543]

Hasegawa T, Hall CJ, Crosier PS, Abe G, Kawakami K, Kudo A, and Kawakami A (2017). Transient inflammatory response mediated by interleukin-1β is required for proper regeneration in zebrafish fin fold. ELife 6.

He Q, Zhang C, Wang L, Zhang P, Ma D, Lv J, and Liu F (2015). Inflammatory signaling regulates hematopoietic stem and progenitor cell emergence in vertebrates. Blood 125, 1098–1106. [PubMed: 25540193]

He Y, Hara H, and Núñez G (2016). Mechanism and Regulation of NLRP3 Inflammasome Activation. Trends Biochem. Sci 41, 1012–1021. [PubMed: 27669650]

Hogan BM, Bos FL, Bussmann J, Witte M, Chi NC, Duckers HJ, and Schulte-Merker S (2009). Ccbe1 is required for embryonic lymphangiogenesis and venous sprouting. Nat. Genet 41, 396–398. [PubMed: 19287381]

Hornung V, Bauernfeind F, Halle A, Samstad EO, Kono H, Rock KL, Fitzgerald KA, and Latz E (2008). Silica crystals and aluminum salts activate the NALP3 inflammasome through phagosomal destabilization. Nat. Immunol 9, 847–856. [PubMed: 18604214]

Hughes MM, and O'Neill LAJ (2018). Metabolic regulation of NLRP3. Immunol. Rev 281, 88–98. [PubMed: 29247992]

Imtiyaz HZ, and Simon MC (2010). Hypoxia-inducible factors as essential regulators of inflammation. Curr. Top. Microbiol. Immunol 345, 105–120. [PubMed: 20517715]

Ivanovs A, Rybtsov S, Ng ES, Stanley EG, Elefanty AG, and Medvinsky A (2017). Human haematopoietic stem cell development: from the embryo to the dish. Development 144, 2323–2337. [PubMed: 28676567]

Jeong J-Y, Einhorn Z, Mathur P, Chen L, Lee S, Kawakami K, and Guo S (2007). Patterning the zebrafish diencephalon by the conserved zinc-finger protein Fezl. Development 134, 127–136. [PubMed: 17164418]

Jo E-K, Kim JK, Shin D-M, and Sasakawa C (2016). Molecular mechanisms regulating NLRP3 inflammasome activation. Cell. Mol. Immunol 13, 148–159. [PubMed: 26549800]

Jurczyk A, Roy N, Bajwa R, Gut P, Lipson K, Yang C, Covassin L, Racki WJ, Rossini AA, Phillips N, et al. (2011). Dynamic glucoregulation and mammalian-like responses to metabolic and developmental disruption in zebrafish. Gen. Comp. Endocrinol 170, 334–345. [PubMed: 20965191]

Kikuchi K, Holdway JE, Major RJ, Blum N, Dahn RD, Begemann G, and Poss KD (2011). Retinoic acid production by endocardium and epicardium is an injury response essential for zebrafish heart regeneration. Dev. Cell 20, 397–404. [PubMed: 21397850]

King KY, and Goodell MA (2011). Inflammatory modulation of HSCs: viewing the HSC as a foundation for the immune response. Nat. Rev. Immunol 11, 685–692. [PubMed: 21904387]

Kissa K, and Herbomel P (2010). Blood stem cells emerge from aortic endothelium by a novel type of cell transition. Nature 464, 112–115. [PubMed: 20154732]

Kuri P, Schieber NL, Thumberger T, Wittbrodt J, Schwab Y, and Leptin M (2017). Dynamics of in vivo ASC speck formation. J. Cell Biol 216, 2891–2909. [PubMed: 28701426]

Kwan KM, Fujimoto E, Grabher C, Mangum BD, Hardy ME, Campbell DS, Parant JM, Yost HJ, and Kanki JP (2007). The Tol2kit: A multisite gateway-based construction kit forTol2 transposon transgenesis constructs. Dev. Dyn 236, 3088–3099. [PubMed: 17937395]

Laing KJ, Purcell MK, Winton JR, and Hansen JD (2008). A genomic view of the NOD-like receptor family in teleost fish: identification of a novel NLR subfamily in zebrafish. BMC Evol. Biol 8, 42. [PubMed: 18254971]

Lam EYN, Hall CJ, Crosier PS, Crosier KE, and Flores MV (2010). Live imaging of Runx1 expression in the dorsal aorta tracks the emergence of blood progenitors from endothelial cells. Blood 116, 909–914. [PubMed: 20453160]

Langenau DM, Traver D, Ferrando AA, Kutok JL, Aster JC, Kanki JP, Lin S, Prochownik E, Trede NS, Zon LI, et al. (2003). Myc-Induced T Cell Leukemia in Transgenic Zebrafish. Science 299, 887–890. [PubMed: 12574629]

Lee H-M, Kim J-J, Kim HJ, Shong M, Ku BJ, and Jo E-K (2013). Upregulated NLRP3 Inflammasome Activation in Patients With Type 2 Diabetes. Diabetes 62, 194–204. [PubMed: 23086037]

Li J, Gao K, Shao T, Fan D, Hu C, Sun C, Dong W, Lin A, Xiang L, and Shao J (2018). Characterization of an NLRP1 Inflammasome from Zebrafish Reveals a Unique Sequential Activation Mechanism Underlying Inflammatory Caspases in Ancient Vertebrates. J. Immunol 201, 1946–1966. [PubMed: 30150286]

Li J-Y, Wang Y-Y, Shao T, Fan D-D, Lin A-F, Xiang L-X, and Shao J-Z (2020). The zebrafish NLRP3 inflammasome has functional roles in ASC-dependent interleukin-1β maturation and gasdermin E-mediated pyroptosis. J. Biol. Chem 295, 1120–1141. [PubMed: 31852739]

Li P, Lahvic JL, Binder V, Pugach EK, Riley EB, Tamplin OJ, Panigrahy D, Bowman TV, Barrett FG, Heffner GC, et al. (2015). Epoxyeicosatrienoic acids enhance embryonic haematopoiesis and adult marrow engraftment. Nature 523, 468–471. [PubMed: 26201599]

Li Y, Esain V, Teng L, Xu J, Kwan W, Frost IM, Yzaguirre AD, Cai X, Cortes M, Maijenburg MW, et al. (2014). Inflammatory signaling regulates embryonic hematopoietic stem and progenitor cell production. Genes Dev. 28, 2597–2612. [PubMed: 25395663]

Lim S-E, Esain V, Kwan W, Theodore LN, Cortes M, Frost IM, Liu SY, and North TE (2017). HIF1α-induced PDGFRβ signaling promotes developmental HSC production via IL-6 activation. Exp. Hematol 46, 83–95.e6. [PubMed: 27751871]

Lin H-F, Traver D, Zhu H, Dooley K, Paw BH, Zon LI, and Handin RI (2005). Analysis of thrombocyte development in CD41-GFP transgenic zebrafish. Blood 106, 3803–3810. [PubMed: 16099879]

López-Muñoz A, Sepulcre MP, Roca FJ, Figueras A, Meseguer J, and Mulero V (2011). Evolutionary conserved pro-inflammatory and antigen presentation functions of zebrafish IFNγ revealed by transcriptomic and functional analysis. Mol. Immunol 48, 1073–1083. [PubMed: 21354627]

Ma D, Zhang J, Lin H, Italiano J, and Handin RI (2011). The identification and characterization of zebrafish hematopoietic stem cells. Blood 118, 289–297. [PubMed: 21586750]

Mariani SA, Li Z, Rice S, Krieg C, Fragkogianni S, Robinson M, Vink CS, Pollard JW, and Dzierzak E (2019). Pro-inflammatory Aorta-Associated Macrophages Are Involved in Embryonic Development of Hematopoietic Stem Cells. Immunity 50, 1439–1452.e5.

Masters SL, Dunne A, Subramanian SL, Hull RL, Tannahill GM, Sharp FA, Becker C, Franchi L, Yoshihara E, Chen Z, et al. (2010). Activation of the NLRP3 inflammasome by islet amyloid polypeptide provides a mechanism for enhanced IL-1β in type 2 diabetes. Nat. Immunol 11, 897–904. [PubMed: 20835230]

Masters SL, Gerlic M, Metcalf D, Preston S, Pellegrini M, O'Donnell JA, McArthur K, Baldwin TM, Chevrier S, Nowell CJ, et al. (2012). NLRP1 Inflammasome Activation Induces Pyroptosis of Hematopoietic Progenitor Cells. Immunity 37, 1009–1023. [PubMed: 23219391]

Masumoto J, Zhou W, Chen FF, Su F, Kuwada JY, Hidaka E, Katsuyama T, Sagara J, Taniguchi S, Ngo-Hazelett P, et al. (2003). Caspy, a zebrafish caspase, activated by ASC oligomerization is required for pharyngeal arch development. J. Biol. Chem 278, 4268–4276. [PubMed: 12464617]

Matty MA, Knudsen DR, Walton EM, Beerman RW, Cronan MR, Pyle CJ, Hernandez RE, and Tobin DM (2019). Potentiation of P2RX7 as a host-directed strategy for control of mycobacterial infection. ELife 8.

McGrath KE, Frame JM, Fegan KH, Bowen JR, Conway SJ, Catherman SC, Kingsley PD, Koniski AD, and Palis J (2015). Distinct Sources of Hematopoietic Progenitors Emerge before HSCs and Provide Functional Blood Cells in the Mammalian Embryo. Cell Rep. 11, 1892–1904. [PubMed: 26095363]

Medvinsky A, Rybtsov S, and Taoudi S (2011). Embryonic origin of the adult hematopoietic system: advances and questions. Development 138, 1017–1031. [PubMed: 21343360]

Mirantes C, Passegué E, and Pietras EM (2014). Pro-inflammatory cytokines: Emerging players regulating HSC function in normal and diseased hematopoiesis. Exp. Cell Res 329, 248–254. [PubMed: 25149680]

Moon J-S, Hisata S, Park M-A, DeNicola GM, Ryter SW, Nakahira K, and Choi AMK (2015). mTORC1-Induced HK1-Dependent Glycolysis Regulates NLRP3 Inflammasome Activation. Cell Rep. 12, 102–115. [PubMed: 26119735]

Navarro-Montero O, Ayllon V, Lamolda M, López-Onieva L, Montes R, Bueno C, Ng E, Guerrero-Carreno X, Romero T, Romero-Moya D, et al. (2017). RUNX1c Regulates Hematopoietic Differentiation of Human Pluripotent Stem Cells Possibly in Cooperation with Proinflammatory Signaling: RUNX1c Promotes Human Embryonic Hematopoiesis. STEM CELLS 35, 2253–2266. [PubMed: 28869683]

Nemeth E, Rivera S, Gabayan V, Keller C, Taudorf S, Pedersen BK, and Ganz T (2004). IL-6 mediates hypoferremia of inflammation by inducing the synthesis of the iron regulatory hormone hepcidin. J. Clin. Invest 113, 1271–1276. [PubMed: 15124018]

Nguyen-Chi M, Phan QT, Gonzalez C, Dubremetz J-F, Levraud J-P, and Lutfalla G (2014). Transient infection of the zebrafish notochord with E. coli induces chronic inflammation. Dis. Model. Mech 7, 871–882. [PubMed: 24973754]

North TE, Goessling W, Walkley CR, Lengerke C, Kopani KR, Lord AM, Weber GJ, Bowman TV, Jang I-H, Grosser T, et al. (2007). Prostaglandin E2 regulates vertebrate haematopoietic stem cell homeostasis. Nature 447, 1007–1011. [PubMed: 17581586]

North TE, Goessling W, Peeters M, Li P, Ceol C, Lord AM, Weber GJ, Harris J, Cutting CC, Huang P, et al. (2009). Hematopoietic Stem Cell Development Is Dependent on Blood Flow. Cell 137, 736–748. [PubMed: 19450519]

Ogryzko NV, Lewis A, Wilson HL, Meijer AH, Renshaw SA, and Elks PM (2019). Hif-1α–Induced Expression of Il-1β Protects against Mycobacterial Infection in Zebrafish. J. Immunol 202, 494–502. [PubMed: 30552162]

Orelio C, Haak E, Peeters M, and Dzierzak E (2008). Interleukin-1-mediated hematopoietic cell regulation in the aorta-gonad-mesonephros region of the mouse embryo. Blood 112, 4895–4904. [PubMed: 18805969]

Orelio C, Peeters M, Haak E, van der Horn K, and Dzierzak E (2009). Interleukin-1 regulates hematopoietic progenitor and stem cells in the midgestation mouse fetal liver. Haematologica 94, 462–469. [PubMed: 19229053]

Palha N, Guivel-Benhassine F, Briolat V, Lutfalla G, Sourisseau M, Ellett F, Wang C-H, Lieschke GJ, Herbomel P, Schwartz O, et al. (2013). Real-Time Whole-Body Visualization of Chikungunya Virus Infection and Host Interferon Response in Zebrafish. PLOS Pathog. 9, e1003619. [PubMed: 24039582]

Patel MN, Carroll RG, Galván-Peña S, Mills EL, Olden R, Triantafilou M, Wolf AI, Bryant CE, Triantafilou K, and Masters SL (2017). Inflammasome Priming in Sterile Inflammatory Disease. Trends Mol. Med 23, 165–180. [PubMed: 28109721]

Pietras EM, Mirantes-Barbeito C, Fong S, Loeffler D, Kovtonyuk LV, Zhang S, Lakshminarasimhan R, Chin CP, Techner J-M, Will B, et al. (2016). Chronic interleukin-1 exposure drives haematopoietic stem cells towards precocious myeloid differentiation at the expense of self-renewal. Nat. Cell Biol 18, 607–618. [PubMed: 27111842]

Progatzky F, Sangha NJ, Yoshida N, McBrien M, Cheung J, Shia A, Scott J, Marchesi JR, Lamb JR, Bugeon L, et al. (2014). Dietary cholesterol directly induces acute inflammasome-dependent intestinal inflammation. Nat. Commun 5, 5864. [PubMed: 25536194]

Renshaw SA, Loynes CA, Trushell DMI, Elworthy S, Ingham PW, and Whyte MKB (2006). A transgenic zebrafish model of neutrophilic inflammation. Blood 108, 3976–3978. [PubMed: 16926288]

Rock KL, Latz E, Ontiveros F, and Kono H (2010). The Sterile Inflammatory Response. Annu. Rev. Immunol 28, 321–342. [PubMed: 20307211]

Sawamiphak S, Kontarakis Z, and Stainier DYR (2014). Interferon gamma signaling positively regulates hematopoietic stem cell emergence. Dev. Cell 31, 640–653. [PubMed: 25490269]

Schindelin J, Arganda-Carreras I, Frise E, Kaynig V, Longair M, Pietzsch T, Preibisch S, Rueden C, Saalfeld S, Schmid B, et al. (2012). Fiji: an open-source platform for biological-image analysis. Nat. Methods 9, 676–682. [PubMed: 22743772]

Sharif O, Bolshakov VN, Raines S, Newham P, and Perkins ND (2007). Transcriptional profiling of the LPS induced NF-κB response in macrophages. BMC Immunol. 8, 1. [PubMed: 17222336]

Sieger D, Stein C, Neifer D, van der Sar AM, and Leptin M (2009). The role of gamma interferon in innate immunity in the zebrafish embryo. Dis. Model. Mech 2, 571–581. [PubMed: 19779068]

Son M-Y, Kwak JE, Seol B, Lee DY, Jeon H, and Cho YS (2015). A novel human model of the neurodegenerative disease GM1 gangliosidosis using induced pluripotent stem cells demonstrates inflammasome activation. J. Pathol 237, 98–110. [PubMed: 25925601]

Spandidos A, Wang X, Wang H, and Seed B (2010). PrimerBank: a resource of human and mouse PCR primer pairs for gene expression detection and quantification. Nucleic Acids Res. 38, D792–D799. [PubMed: 19906719]

Sturgeon CM, Ditadi A, Awong G, Kennedy M, and Keller G (2014). Wnt signaling controls the specification of definitive and primitive hematopoiesis from human pluripotent stem cells. Nat. Biotechnol 32, 554–561. [PubMed: 24837661]

Sugimura R, Jha DK, Han A, Soria-Valles C, da Rocha EL, Lu Y-F, Goettel JA, Serrao E, Rowe RG, Malleshaiah M, et al. (2017). Haematopoietic stem and progenitor cells from human pluripotent stem cells. Nature 545, 432–438. [PubMed: 28514439]

Sugiyama M, Sakaue-Sawano A, Iimura T, Fukami K, Kitaguchi T, Kawakami K, Okamoto H, Higashijima S.-i, and Miyawaki A (2009). Illuminating cell-cycle progression in the developing zebrafish embryo. Proc. Natl. Acad. Sci 106, 20812–20817. [PubMed: 19923430]

Sun S, Ganchi P, Ballard D, and Greene W (1993). NF-kappa B controls expression of inhibitor I kappa B alpha: evidence for an inducible autoregulatory pathway. Science 259, 1912–1915. [PubMed: 8096091]

Takizawa H, Regoes RR, Boddupalli CS, Bonhoeffer S, and Manz MG (2011). Dynamic variation in cycling of hematopoietic stem cells in steady state and inflammation. J. Exp. Med 208, 273–284. [PubMed: 21300914]

Tannahill GM, Curtis AM, Adamik J, Palsson-McDermott EM, McGettrick AF, Goel G, Frezza C, Bernard NJ, Kelly B, Foley NH, et al. (2013). Succinate is an inflammatory signal that induces IL-1β through HIF-1α. Nature 496, 238–242. [PubMed: 23535595]

Tian Y, Xu J, Feng S, He S, Zhao S, Zhu L, Jin W, Dai Y, Luo L, Qu JY, et al. (2017). The first wave of T lymphopoiesis in zebrafish arises from aorta endothelium independent of hematopoietic stem cells. J. Exp. Med 214, 3347–3360. [PubMed: 28931624]

Tirziu D, Jaba IM, Yu P, Larrivée B, Coon BG, Cristofaro B, Zhuang ZW, Lanahan AA, Schwartz MA, Eichmann A, et al. (2012). Endothelial NFκB - Dependent Regulation of Arteriogenesis and Branching. Circulation 126, 2589–2600. [PubMed: 23091063]

Traver D, Paw BH, Poss KD, Penberthy WT, Lin S, and Zon LI (2003). Transplantation and in vivo imaging of multilineage engraftment in zebrafish bloodless mutants. Nat. Immunol 4, 1238–1246. [PubMed: 14608381]

Tseng HHL, Vong CT, Kwan YW, Lee SM-Y, and Hoi MPM (2016). TRPM2 regulates TXNIP-mediated NLRP3 inflammasome activation via interaction with p47 phox under high glucose in human monocytic cells. Sci. Rep 6, 35016. [PubMed: 27731349]

Tsuchiya S, Yamabe M, Yamaguchi Y, Kobayashi Y, Konno T, and Tada K (1980). Establishment and characterization of a human acute monocytic leukemia cell line (THP-1). Int. J. Cancer 26, 171–176. [PubMed: 6970727]

Tyrkalska SD, Pérez-Oliva AB, Rodríguez-Ruiz L, Martínez-Morcillo FJ, Alcaraz-Pérez F, Martínez-Navarro FJ, Lachaud C, Ahmed N, Schroeder T, Pardo-Sánchez I, et al. (2019). Inflammasome Regulates Hematopoiesis through Cleavage of the Master Erythroid Transcription Factor GATA1. Immunity 51, 50–63.e5. [PubMed: 31174991]

Vojtech LN, Scharping N, Woodson JC, and Hansen JD (2012). Roles of Inflammatory Caspases during Processing of Zebrafish Interleukin-1β in Francisella noatunensis Infection. Infect. Immun 80, 2878–2885. [PubMed: 22689811]

Walton EM, Cronan MR, Beerman RW, and Tobin DM (2015). The Macrophage-Specific Promoter mfap4 Allows Live, Long-Term Analysis of Macrophage Behavior during Mycobacterial Infection in Zebrafish. PLOS ONE 10, e0138949.

Zhao S, and Fernald RD (2005). Comprehensive Algorithm for Quantitative Real-Time Polymerase Chain Reaction. J. Comput. Biol. J. Comput. Mol. Cell Biol 12, 1047–1064.

Zhao JL, Ma C, O'Connell RM, Mehta A, DiLoreto R, Heath JR, and Baltimore D (2014). Conversion of Danger Signals into Cytokine Signals by Hematopoietic Stem and Progenitor Cells for Regulation of Stress-Induced Hematopoiesis. Cell Stem Cell 14, 445–459. [PubMed: 24561084]

Highlights:

- Developmental metabolic shifts prime inflammasome-associated *il1b* expression *in vivo*
- Loss of inflammasome function inhibits HSPC production in the zebrafish embryo
- IL1β^{+} macrophages promote production of Il1rl1^{+} HSPCs via inflammasome action *in vivo*
- Inflammasome activation enhances HSPC production in human hemogenic cultures

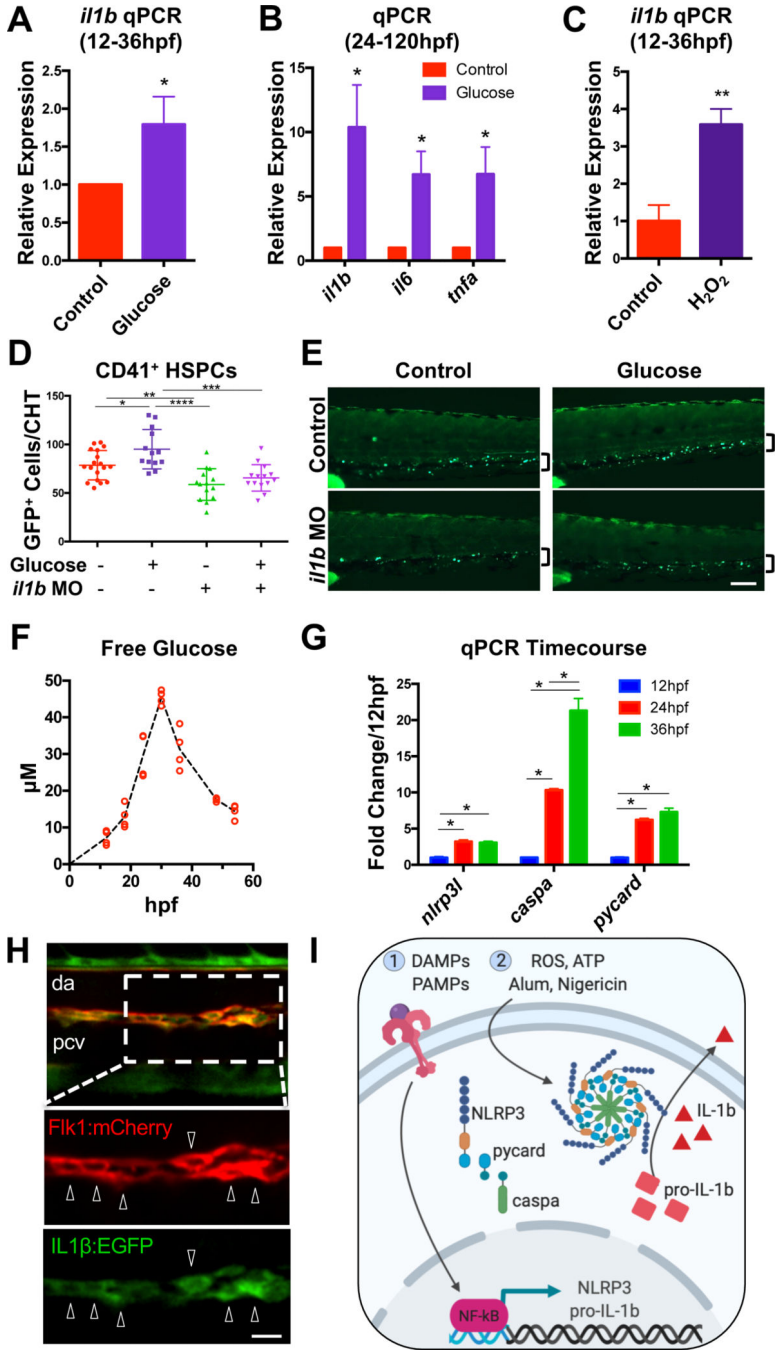

Figure 1. Metabolic stimulation promotes expression of inflammatory cytokines.

(A) Glucose (1% in E3 water, 12–36hpf) increases *il1b* expression during HSPC specification (n=8, mean ±SEM) and (B) expansion (1% glucose from 24–120hpf; n=4, mean ±SEM). (C) Reactive oxygen species (0.005% H_2O_2; 12–36hpf) increases *il1b* expression. (n=4, mean ±SEM). (D,E) Morpholino oligonucleotides (MO) targeting *il1b* prevents glucose (12–48hpf) from increasing $CD41^+$ HSPCs in the CHT. Significance determined by ANOVA with Tukey's multiple comparison test. Scale bar, 100μm. (F) Glucose levels measured in pooled embryo lysates from 2 independent clutches over

developmental time. Each point represents the glucose concentration from 24 embryos. (G) Inflammasome component expression over developmental time (n=4, mean ±SEM). (H) IL1β:EGFP expression (bottom inset, arrowheads) in the *Tg(il1b:EGFP;flk1:mCherry)* dorsal aorta (da) at 36hpf. Pcv, posterior cardinal vein. Scale bar, 10μm. (I) NLRP3 inflammasome model. Image created with BioRender.com. *P<0.05, **P<0.01, ***P<0.001; ****P<0.0001. See also Figure S1.

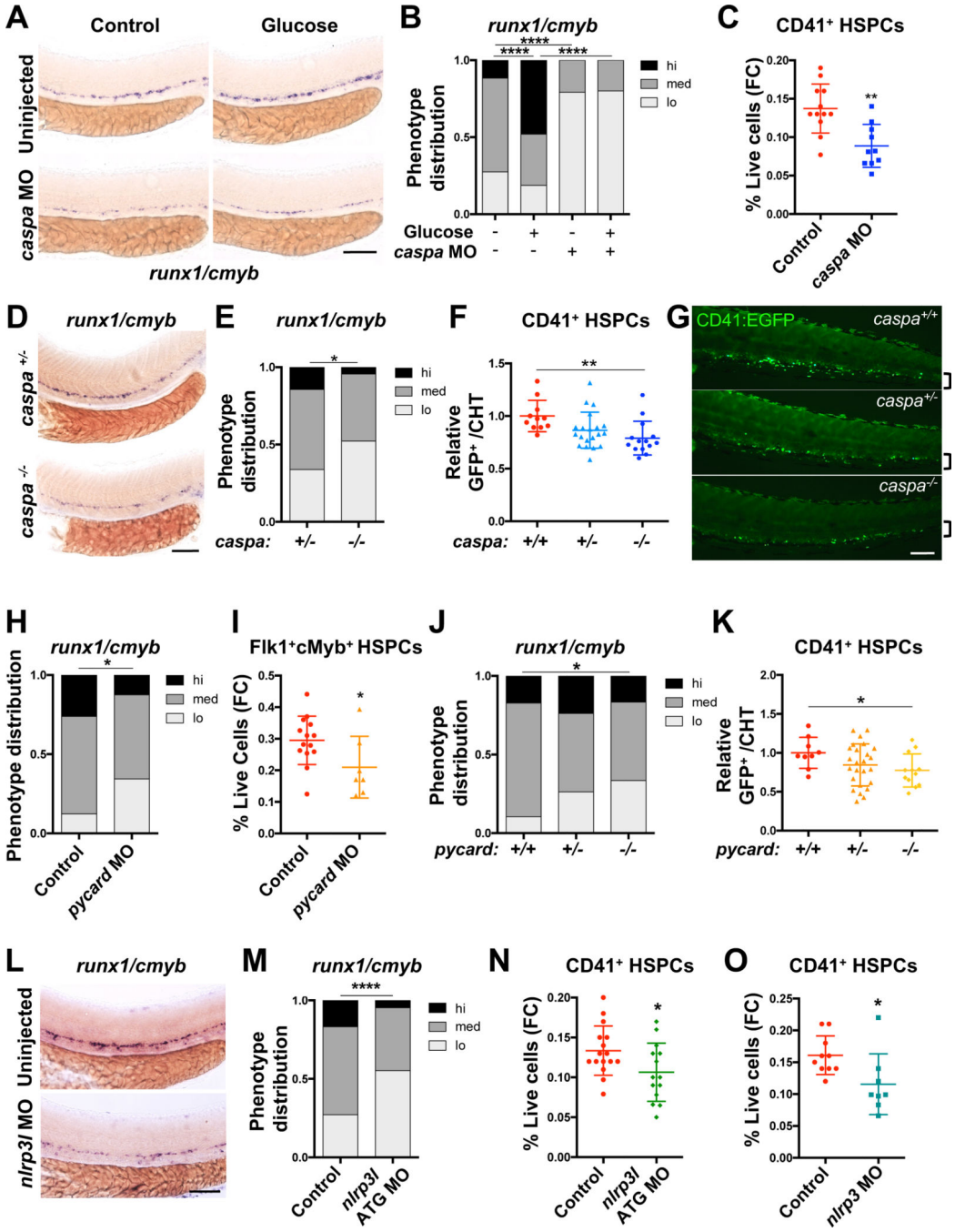

Figure 2. Inflammasome action regulates HSPC formation.

(A-B) Expression of *runx1/cmyb* in embryos with or without morpholino (MO)-mediated *caspa* knockdown or 1% glucose treatment (12–36hpf) assessed by WISH. (C) *caspa* knockdown reduces frequency of CD41:EGFP^{+} HSPCs by flow cytometry (FC) at 48hpf. (D-E) *runx1/cmyb* WISH of *caspa*$^{-/-}$ aortas compared with *caspa*$^{+/-}$ embryos at 36hpf. (F-G) CD41:EGFP^{+} HSPCs in the CHT of embryos from *caspa*$^{+/-}$ incrosses at 48hpf. Counts were normalized relative to *caspa*$^{+/+}$ embryos for each clutch. Significance was determined by Tukey's multiple comparison test. (H-I) *pycard* knockdown reduces *runx1/cmyb*

expression by WISH (36hpf), and the frequency of HSPCs in *Tg(flk1:dsRed;cmyb:egfp)* embryos by flow cytometry (48hpf). (J) *runx1/cmyb* WISH in *pycard*$^{-/-}$ embryos compared with stage-matched *pycard*$^{+/+}$ and *pycard*$^{+/-}$ embryos. (K) CD41^{+} HSPCs in the CHT of embryos from *pycard*$^{+/-}$ incrosses. Counts were normalized relative to *pycard*$^{+/+}$ embryos for each clutch. Significance was determined by Fisher's LSD test. (L-M) *nlrp3l* knockdown reduces *runx1/cmyb* by WISH and (N) the frequency of HSPCs assayed by flow cytometry at 48hpf. (O) *nlrp3* knockdown reduces the frequency of CD41^{+} HSPCs at 48hpf. *P<0.05, **P<0.01, ***P<0.001, ****P<0.0001. Scale bars, 100μm. See also Figure S2.

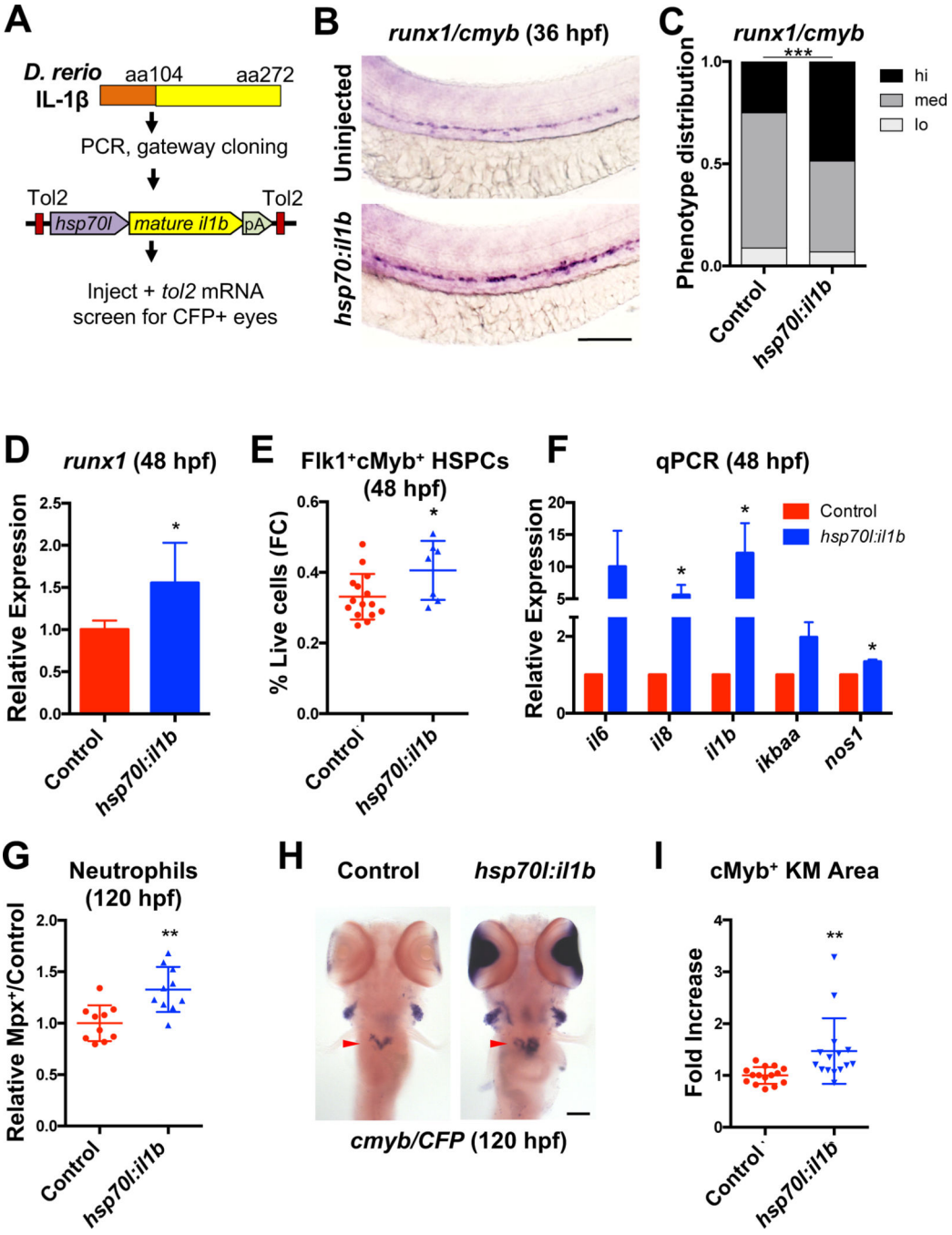

Figure 3. IL1β mediates HSPC production.

(A) Generation of *Tg(hsp70l:il1b)* embryos. (B-C) *il1b* overexpression (actIL1β; 32hpf) promotes *runx1/cmyb* expression at 36hpf in chimeric injected animals. (D) actIL1β induces *runx1* in whole *Tg(hsp70l:il1b)* embryos by qPCR (48hpf, n=5, mean ±SEM). (E) HSPCs quantified by flow cytometry (FC) in *Tg(flk1:dsRed;cmyb:GFP;hsp70l:il1b)* embryos compared with actIL1β^{-} controls (48hpf). (F) actIL1β (32hpf) induces expression of *il1b* and common targets (n>3, 48hpf, mean ±SEM). (G) Relative frequency of neutrophils in 120hpf *Tg(mpx:GFP;hsp70l:il1b)* embryos heat-shocked at 32hpf. (H-I) Kidney marrow

area (arrow), denoted by *cmyb* expression, is proportionally increased at 120hpf after actIL1β induction at 32hpf. CFP eye signal was used to identify presence of the *hsp70l:il1b* transgene. Scale bars, 100μm. *P<0.05, **P<0.01. See also Figure S3.

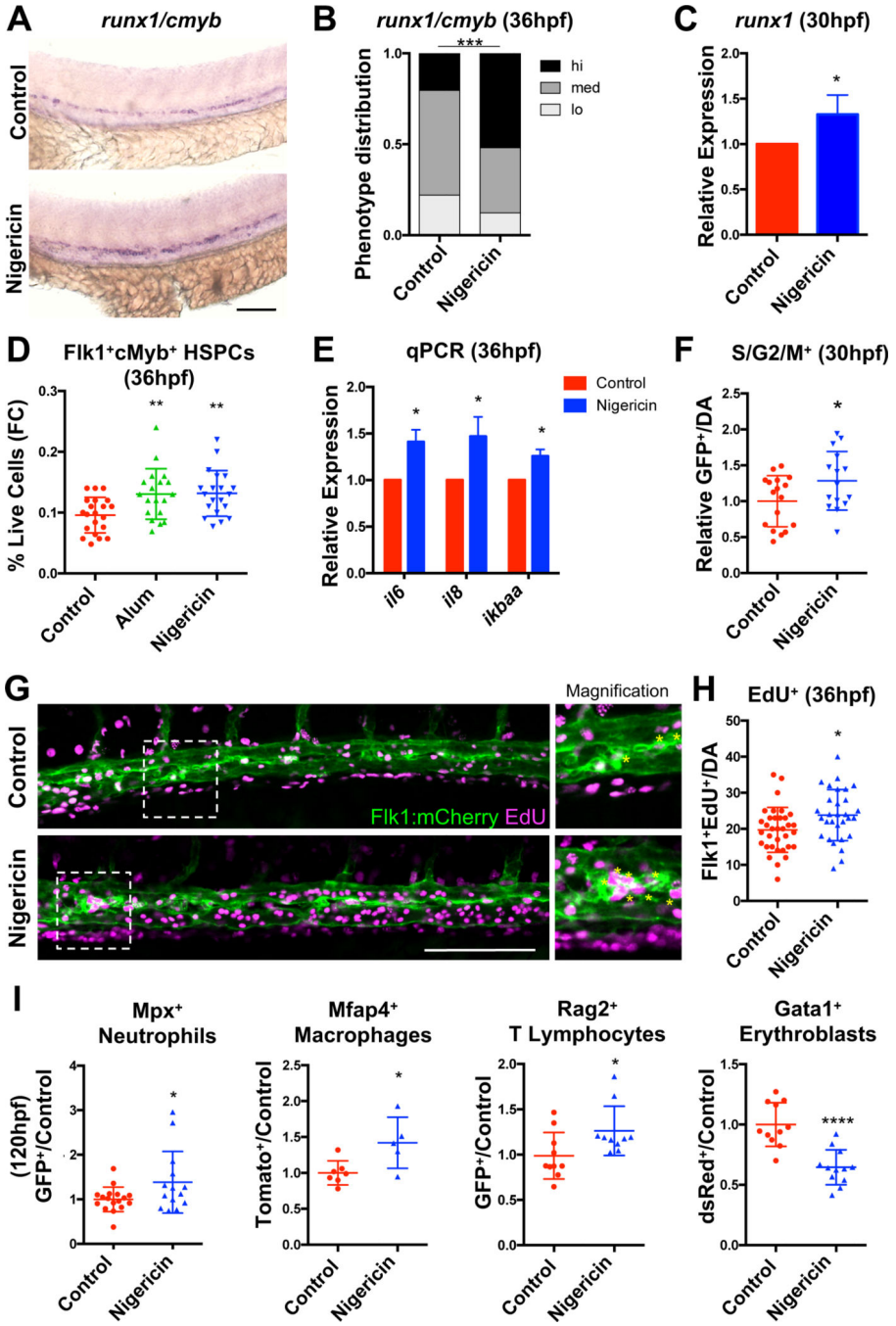

Figure 4. HSPC production is enhanced by inflammasome activation.

(A-B) Inflammasome stimulation (12–36hpf) promotes *runx1/cmyb* expression by WISH. (C) *runx1* qPCR (n=4, mean ±SEM). (D) Nigericin or Alum (12–36hpf) increased HSPCs by flow cytometry (FC). Significance was determined by ANOVA with Dunnett's post-hoc test. (E) qPCR of IL1β target genes (n=6, mean ±SEM). (F) Relative numbers of S/G2/M^{+} cells in *Tg(EF1a:mAG-zGem(1/100))* aortas with nigericin stimulation (12–30hpf) (DA; dorsal aorta; Fold change calculated within each clutch). (G-H) Numbers of Flk1^{+}EdU^{+} cells in the aortic floor in 36hpf *Tg(flk1:mCherry)* embryos labeled with EdU antibody. Asterisks

in inset signify positive cells. (I) The proportion of Mpx^+ neutrophils, $Mfap4^+$ macrophages, $Rag2^+$ lymphocytes, and $Gata1^+$ erythroblasts in transgenic embryos was assessed with prolonged nigericin stimulation (24–120hpf) by flow cytometry. *P<0.05, **P<0.01, ****P<0.0001. Scale bars, 100μm. See also Figure S4.

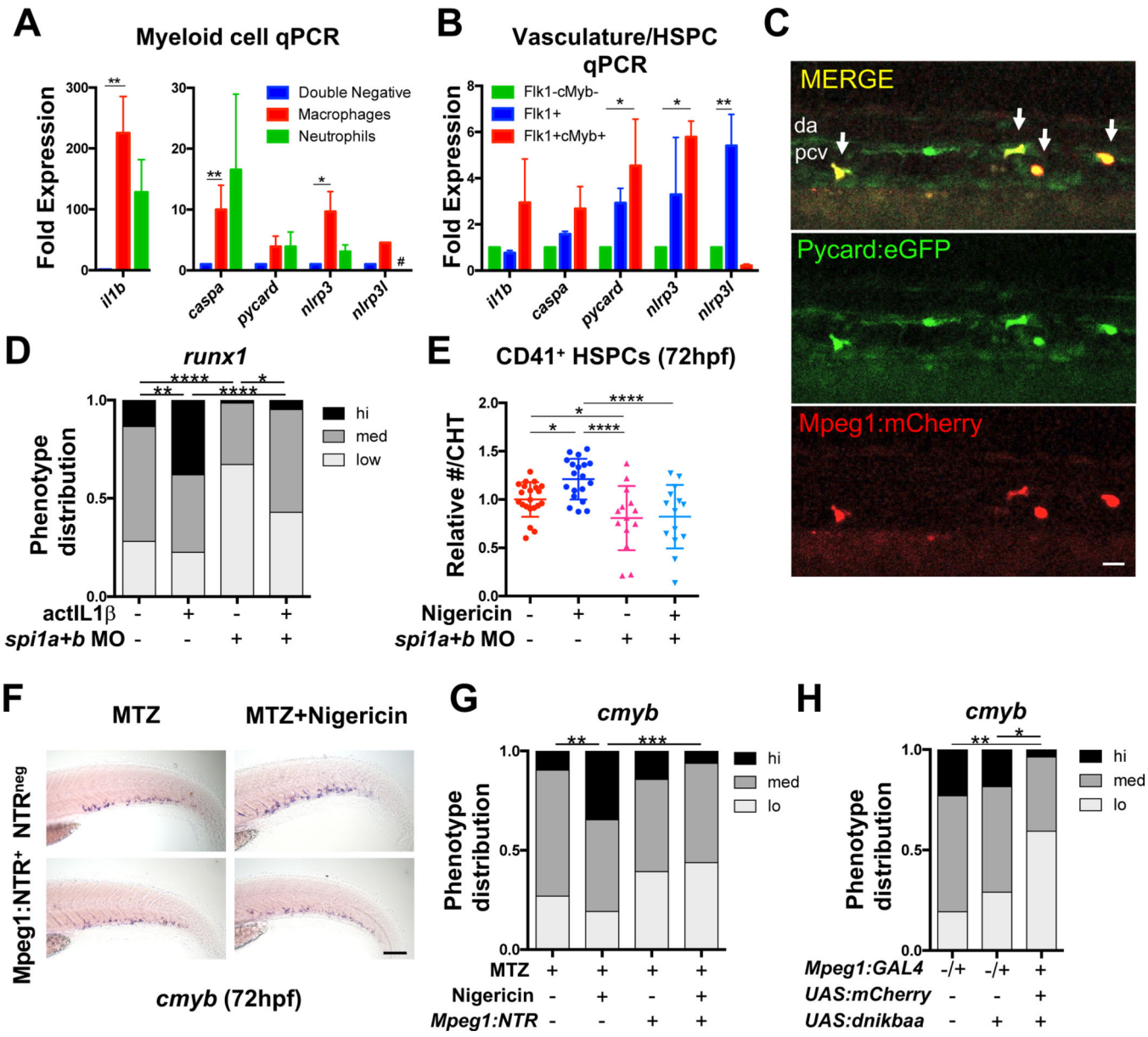

Figure 5. Myeloid cells are required to mediate the effects of the inflammasome on HSPCs.

(A) Inflammasome component qPCR in sorted Mpeg1^{+} macrophages and Mpx^{+} neutrophils relative to the Mpeg1^{-}Mpx^{-} fraction in 48hpf *Tg(mpeg1:GAL4;UAS:NTR-mCherry;mpx:GFP)* embryos (mean ±SEM, n>3, Holm-Sidak testing). Mpx^{+} v. Negative; *P*=0.056; #, below detection. (B) Inflammasome component qPCR in sorted Flk1^{+} vasculature and Flk^{+}cMyb^{+} HSPCs relative to the Flk1^{-}cMyb^{-} fraction at 48hpf (mean ±SEM, n=4, Holm-Sidak testing). (C) Co-expression of EGFP and mCherry (arrows) beneath the dorsal aorta (DA) of 30hpf *Tg(mpeg1:mCherry;pycard:pycard-EGFP)* embryos. PCV, posterior cardinal vein. Scale bar, 20μm. (D) Knockdown of *spi1a/spi1b* reduces *runx1* expression by WISH; *il1b* overexpression (24hpf) partially rescues *runx1* expression (36hpf). (E) Loss of *spi1a/spi1b* blocks nigericin-induced expansion of CD41^{+} HSPCs in the CHT (24–72hpf). Significance was determined by ANOVA with Fisher's LSD test. (F-G)

Metronidazole-mediated macrophage ablation (MTZ; 30hpf) in *Tg(mpeg1:GAL4;UAS:nfsB-mCherry)* (Mpeg:NTR) embryos prevents nigericin (30hpf) from increasing *cmyb* CHT expression by WISH (72hpf). Scale bar, 100μm. (H) NFκB blockade in *Tg(mpeg1:GAL4;UAS:nfsB-mCherry;UAS:dnikbaa)* embryos reduces *cmyb* CHT expression by WISH (72hpf). **P*<0.05, ***P*<0.01, ****P*<0.001, *****P*<0.0001. See also Figure S5.

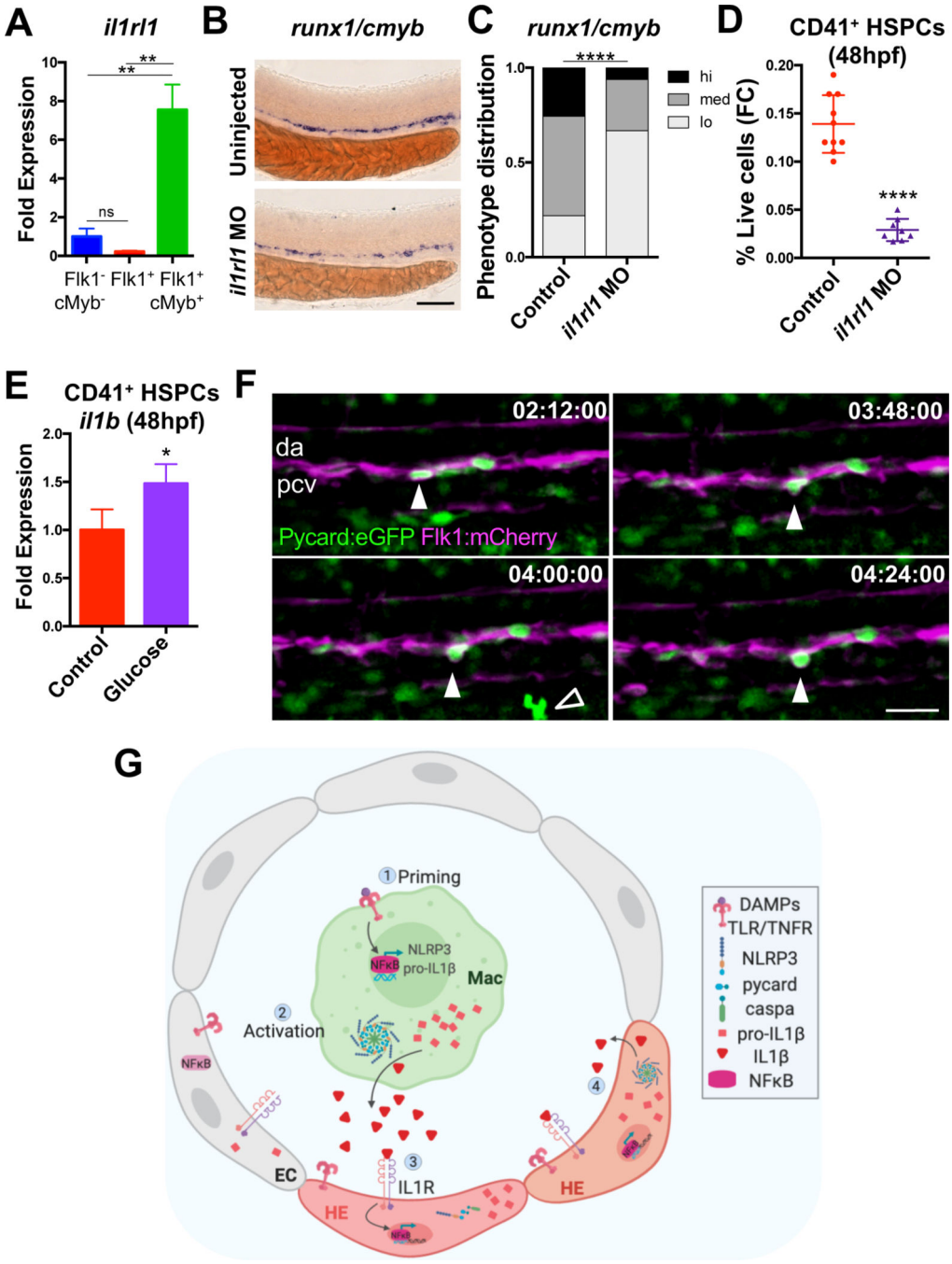

Figure 6. IL1β signals are received by HSPCs to further prime inflammasome activity.

(A) *il1rl1* qPCR in Flk1^{+} vasculature and Flk1^{+}cMyb^{+} HSPCs relative to the Flk1^{-}cMyb^{-} fraction (48hpf). Mean ±SEM, n=3, Holm-Sidak testing. ns, not significant. (B-C) *il1rl1* knockdown reduced *runx1/cmyb* expression in the aorta by WISH (36hpf). Scale bar, 100μm. (D) *il1rl1* knockdown reduces CD41^{+} HSPCs (48hpf) by flow cytometry (FC). (E) *il1b* qPCR in sorted CD41^{+} HSPCs from 1% glucose-treated embryos (12–48hpf). (Mean ±SEM, n=6, 2 independent experiments; fold change was calculated from the average control in each experiment). (F) Sequential time-lapse images demonstrate budding of a

Pycard^{+} cell from the dorsal aorta (DA) of a *Tg(pycard:pycard-EGFP;flk1:mCherry)* embryo (34–36hpf.) Open arrow, putative macrophage. PCV, posterior cardinal vein. Scale bar, 30μm. See also Movie S1. (G) Model of inflammasome regulation of HSPC production. EC, endothelial cell. HE, hemogenic endothelium. Image created from Biorender.com. *P<0.05, **P<0.01, ****P<0.0001. See also Figure S6.

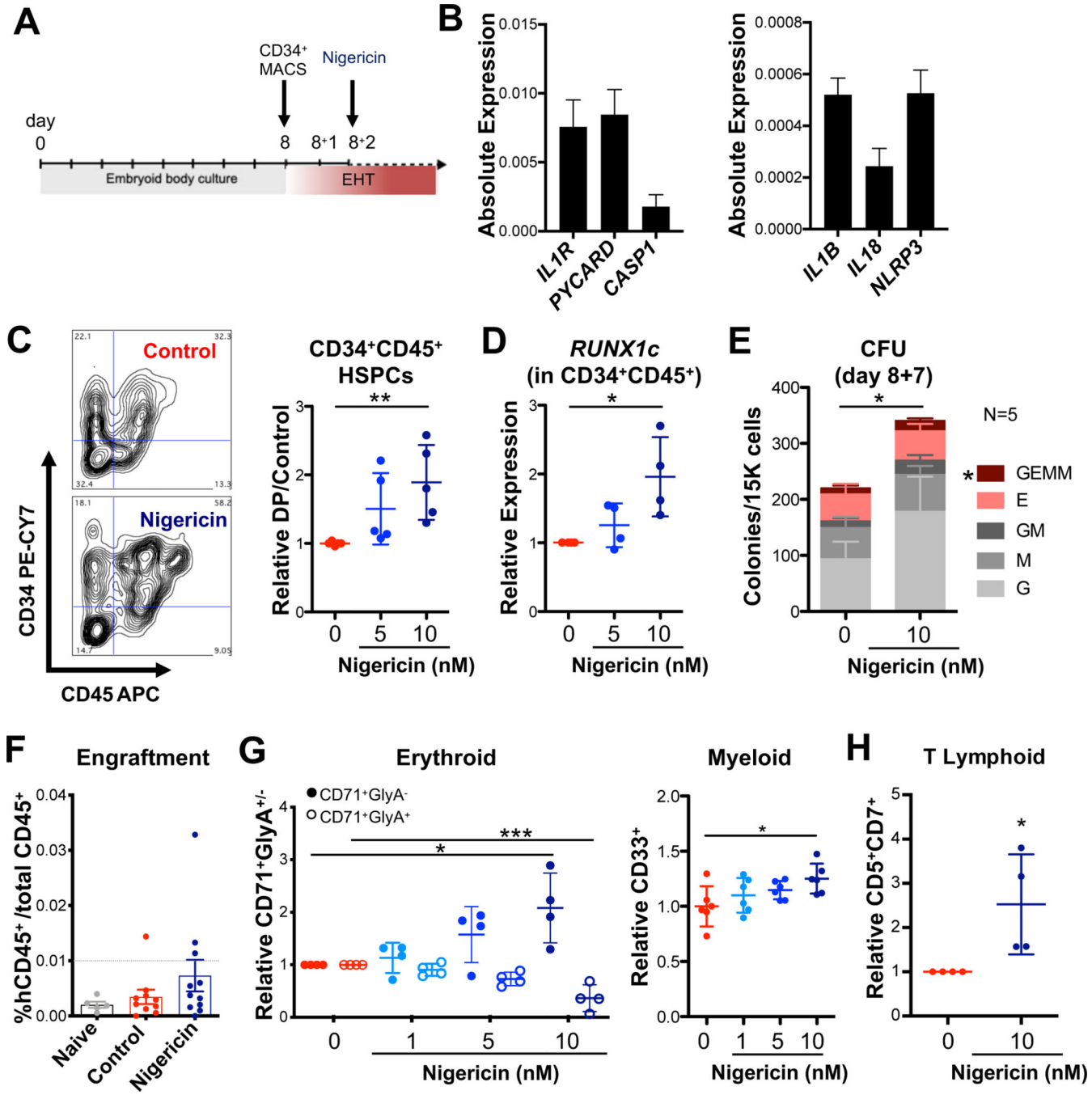

Figure 7. Inflammasome stimulation boosts iPS-derived human HSPC activity *in vitro*.

(A) Schematic of human iPS cell hematopoietic differentiation cultures. Embryoid body-derived cells are enriched for CD34$^+$ hemogenic endothelium (HE) on day 8 of differentiation and subjected to 7 more days of EHT culture. Nigericin (or EtOH to controls) was added on day 2 of EHT. (B) Expression of inflammasome components (relative to *GAPDH*) in day 2 EHT cultures (mean ±SEM, n=3 independent cultures, 3 samples/culture). (C) Nigericin increases CD34$^+$CD45$^+$ cells on day 7, representative FACS plots are shown; n=5 independent differentiation cultures. (D) *RUNX1c* qPCR in CD34$^+$CD45$^+$ cells

from nigericin-treated cultures relative to untreated controls. (E) CFU assays of floating cells harvested on day 7 of EHT culture from 5 differentiations. Nigericin significantly increases both total colonies and GEMM colonies (*P<0.05). (F) Engraftment potential of iPSCs transplanted on day 4 of EHT culture. % of human $CD45^+$ cells was assessed from the total $CD45^+$ population in the bone marrow at 8 weeks post-transplant (mean ±SEM). (G) Nigericin-stimulated cultures yield proportionally fewer $CD71^+GlyA^+$ cells and more $CD33^+$ myeloid cells by day 8. (H) Nigericin stimulation on day 2 of EHT increases pro-T progenitors after 2 weeks. Each point represents the average fold change across multiple wells within a differentiation culture; n=4 independent differentiation cultures. *P<0.05, ***P<0.001. See also Figure S7.

KEY RESOURCES TABLE

REAGENT or RESOURCE	SOURCE	IDENTIFIER
Antibodies		
Human CD34 PE-CY7	Thermo Fisher Scientific	Cat# BDB560710
Human CD45 APC	Beckman Coulter	Cat# IM2473U
Human GLYA/CD235a FITC	Beckman Coulter	Cat# IM2212U
Human CD71 PE	BD Biosciences	Cat# 555537
Human CD19 PE	BioLegend	Cat# 302208
Human CD3 PE-CY7	BioLegend	Cat# 344816
Human CD33 APC	BioLegend	Cat# 303407
Mouse CD45.1 APC-CY7	BioLegend	Cat# 110716
TruStain FcX	BioLegend	Cat# 101320
Human CD34 Microbeads	Miltenyi Biotec	Cat# 130-046-702
Human CD5 PE (M-T701)	BD Biosciences	Cat# 555361
Human CD7 BV510 (UCHT2)	BD Biosciences	Cat# 563381
Anti-digoxigenin-AP Fab Fragments	Millipore Sigma	Cat# 11093274910
Biological Samples		
Human cord blood mononuclear cells (for gating controls)	Stem Cell Technologies	Cat# 70007.1
Corning™ Matrigel™ hESC-Qualified Matrix	ThermoFisher Scientific	Cat# 08774552
CF-1 MEF 4M IRR	ThermoFisher Scientific	Cat# A34181
Chemicals, Peptides, and Recombinant Proteins		
$CoCl_2$	Sigma	Cat# C8661
Alum Crystals	Invivogen	Cat# tlrl-alk
Nigericin	Cayman Chemical	Cat# 11437
Metronidazole	Millipore Sigma	Cat# M3761
Ac-YVAD-CMK	Cayman Chemical	Cat#10014
LPS	Invivogen	Cat# tlrl-eklps
CHIR99021	Stem Cell Technologies	Cat# 72052
SB431542	Stem Cell Technologies	Cat# 72232
Recombinant Human BMP4	PeproTech	Cat# 10779-138
Recombinant Human bFGF	Gibco	Cat# PHG0266
Recombinant Human VEGF	R&D Systems	Cat# 293-VE
Recombinant Human IL6	PeproTech	Cat# 200-06
Recombinant Human IL11	PeproTech	Cat# 200-11
Recombinant Human IGF1	PeproTech	Cat# 100-11
Recombinant Human SCF	PeproTech	Cat# 300-07
Recombinant Human EPO	Epogen	Cat# 55513-144-01
Recombinant Human TPO	PeproTech	Cat# 300-18
Recombinant Human Flt3L	PeproTech	Cat# 300-19

REAGENT or RESOURCE	SOURCE	IDENTIFIER
Recombinant Human IL3	PeproTech	Cat# 200-03
Recombinant human Sonic Hedgehog	PeproTech	Cat# 100-45
Angiotensin II	Millipore Sigma	Cat# A9525-5MG
Losartan Potassium	ThermoFisher Scientific	Cat# 37-985-0
Liberase TM	Millipore Sigma	Cat# 5401127001
Proteinase K	Millipore Sigma	Cat# 3115828001
BCIP	Millipore Sigma	Cat# 11383221001
NBT	Millipore Sigma	Cat# 11383213001
Critical Commercial Assays		
MethoCult™ SF H4636	Stem Cell Technologies	Cat# 04636
StemFlex™ Medium	ThermoFisher Scientific	Cat# A3349401
StemSpan T cell generation kit	Stem Cell Technologies	Cat# 09940
Amplex Red Glucose Assay kit	ThermoFisher Scientific	Cat# A22189
RNEasy Micro Kit	Qiagen	Cat# 74004
RNEasy Plus Micro Kit	Qiagen	Cat# 74034
RNAqueous Kit	ThermoFisher Scientific	Cat# AM1912
Superscript III cDNA Synthesis Supermix	Invitrogen	Cat# 11752050
Superscript VILO cDNA Synthesis kit	Invitrogen	Cat# 11754050
Maxima Reverse Transcriptase kit	ThermoFisher Scientific	Cat# EP0741
Click-iT EdU Cell Proliferation Kit for Imaging, Alexa Fluor 647	Invitrogen	Cat# C10340
LS Columns	Miltenyi Biotec	Cat# 130-042-401
Experimental Models: Cell Lines		
hiPS cells	hESC core facility at Boston Children's Hospital	1157.2
THP-1 monocytes	Invivogen	Cat# thp-null
Experimental Models: Organisms/Strains		
Zebrafish: *Tg(−6.0itga2b:egfp)*^{la2} (*CD41:eGFP*)	(Lin et al., 2005)	ZFIN: ZDB-ALT-051223-4
Zebrafish: *TgBAC(il1b:NTR-EGFP,cryaa:EGFP)*	(Hasegawa et al., 2017)	ZFIN: ZDB-ALT-170531-2
Zebrafish: *Tg(kdrl:Hsa.HRAS-mCherry)*^{s916}	(Hogan et al., 2009)	ZFIN: ZDB-ALT-090506-2
Zebrafish: *Tg(kdrl:dsred2)* (commonly *Flk1:dsred*)	(Kikuchi et al., 2011)	ZFIN: ZDB-ALT-110408-4
Zebrafish: *Tg(cmyb:EGFP)*	(North et al., 2007)	ZFIN: ZDB-ALT-071017-1
Zebrafish: *caspa*^{hdb12}	(Kuri et al., 2017)	ZFIN: ZDB-ALT-180207-12
Zebrafish: *pycard*$^{zf2174/zf2174}$ *(AB)*	(Matty et al., 2019)	ZFIN: ZDB-GENO200316-6
Zebrafish: *Tg(hsp70l:il1b;cryaa:CFP)*	This paper	N/A
Zebrafish: *Tg(mpx:GFP)*	(Renshaw et al., 2006)	ZFIN: ZDB-ALT-070118-2
Zebrafish: *Tg(mfap4:tdTomato-CAAX)*^{xt6}	(Walton et al., 2015)	ZFIN: ZDB-ALT-160122-3
Zebrafish: *Tg(gata1a:dsRed)*	(Traver et al., 2003)	ZFIN: ZDB-ALT-051223-6
Zebrafish: *Tg(UAS:dnnfkbiaa)*^{sd35}	(Espín-Palazón et al., 2014)	ZFIN: ZDB-ALT-151228-5
Zebrafish: *Tg(hsp70l:GAL4)*	(Jeong et al., 2007)	ZFIN: ZDB-ALT-070706-2

REAGENT or RESOURCE	SOURCE	IDENTIFIER
Zebrafish: *Tg(pycard:pycard-EGFP); pycard*^{hdb10Tg}	(Kuri et al., 2017)	ZFIN: ZDB-ALT-180207-11
Zebrafish: *Tg(mpeg1:mCherry)*^{gl23}	(Ellett et al., 2011)	ZFIN: ZDB-ALT-120117-2
Zebrafish: *Tg(mpeg1:EGFP)*^{gl22}	(Ellett et al., 2011)	ZFIN: ZDB-ALT-120117-1
Zebrafish: *Tg(mpeg1:GAL4;UAS:NTR-mCherry)*	(Palha et al., 2013)	ZFIN: ZDB-ALT-120117-3; ZDB-ALT-070316-1
Zebrafish: *Tg(EF1a:mAG-zGem(1/100))*^{rw0410h}*)*	(Sugiyama et al., 2009)	ZFIN: ZDB-ALT-101018-2
Zebrafish: *Tg(rag2:gfp)*	(Langenau et al., 2003)	ZFIN: ZDB-ALT-051111-6
Mouse: NBSGW (NOD.Cg-*Kit*$^{W-41J}$ *Tyr* $^{+}$ *Prkdc*^{scid} *Il2rg*^{tm1Wjl}/ThomJ)	Jackson Laboratory	JAX: 026622
Oligonucleotides		
See Table S1	See Table S1	N/A
Recombinant DNA		
Plasmid: pME-MCS	(Kwan et al., 2007)	Tol2kit v1.2 #237
Plasmid: p3E-polyA	(Kwan et al., 2007)	Tol2kit v1.2 #302
Plasmid: p5E-Hsp70l	(Kwan et al., 2007)	Tol2kit v1.2 #222
Plasmid: p5E-kdrl	Addgene	Cat# 78687
Plasmid: pDestTol2pA2	(Kwan et al., 2007)	Tol2kit v1.2 #394
Plasmid: pCS2FA-Transposase	(Kwan et al., 2007)	Tol2kit v1.2 #396
Plasmid: pDestTol2pA2CryCFP-*hsp70l:il1b*	This paper	N/A
Plasmid: pDestTol2pA2CryCFP-*flk1:il1b*	This paper	N/A
Software and Algorithms		
Fiji	(Schindelin et al., 2012)	https://imagej.net/Fiji
Prism (Version 5, 6, 8)	GraphPad	https://www.graphpad.com/
FlowJo (Version 10)	BD Biosciences	https://www.flowjo.com/
PCRMiner	(Zhao and Fernald, 2005)	http://ewindup.info/miner/home.htm